# AN EXIPLICIT DAMPING SENSITIVITY EXPRESSION FOR POWER SYSTEM STABILIZERS APPLICATIONS IN POWER SYSTEMS

By

Miyada Alnazeer Ezalden Ahmed

Ahmed H. Eltom
Professor of Electrical Engineering
(Committee Chair)

Abdelrahman A. Karrar
Professor of Electrical Engineering
(Committee Co-Chair)

Gary L. Kobet
Adjunct Professor of Electrical Engineering
(Committee Member)

# AN EXPLICIT DAMPING SENSITIVITY EXPRESSION FOR POWER SYSTEM STABILIZERS APPLICATIONS IN POWER SYSTEMS

By

Miyada Alnazeer Ezalden Ahmed

A Thesis Submitted to the Faculty of the University of
Tennessee at Chattanooga in Partial Fulfillment
of the Requirements of the Degree of
Master of Science: Engineering

The University of Tennessee at Chattanooga
Chattanooga, Tennessee

August 2017

# ABSTRACT

Interconnected power systems are subject to low frequency oscillations. These oscillations, if poorly damped, threaten the stability of the system and limit its power transfer capability. Power System Stabilizers (PSS) are widely used to enhance the damping of electromechanical oscillatory modes.

Conventional methods to tune power system stabilizers attempt to provide the required magnitude/phase shift compensation through frequency response or mode sensitivity analysis. However, these methods do not operate directly on the damping sensitivity of the mode.

A novel method to calculate the damping sensitivity has been developed in this work. It operates on mode damping directly to achieve optimum damping for the under-damped oscillatory modes. The proposed method has been used to tune simple stabilizers for the well-known two-area four-machine power system problem and the IEEE9-Bus system. It is compared with results obtained from complex and robust PSS designs, and found to offer comparable outcomes.

TABLE OF CONTENTS

LIST OF TABLES

LIST OF FIGURES

# CHAPTER 1

# INTRODUCTION

## 1.1 Background

Large size synchronous machines that are connected via long transmission lines suffer from low frequency oscillations due to inherent characteristics. This oscillatory behavior endangers the small signal stability of the system and may lead to serious stability problems. One of the most disreputable events was the breakup of the Western Interconnection on August 10, 1996 [1] on account of four poorly damped inter-area oscillations.

To enhance the system stability and mitigate the oscillations, many synchronous generator controllers have been developed. Power System Stabilizer (PSS) is one of the most successful controllers that generate a component of electrical torque in phase with the rotor speed deviation to dampen the rotor oscillations produced by small disturbances.

## 1.2 Problem Statement

The main function of the Power System Stabilizer (PSS) is to improve the damping ratio of the oscillatory modes. To attain this objective, it feeds back a stabilizing signal to the excitation system through lead-phase compensation blocks. The lead phase blocks compensate for the lag-phase generated by the generator and excitation system. Thus, the time constants of the PSS should be tuned wisely to provide as much as required of gain/phase

compensation. Lower compensation leads to poorly damped oscillations. In contrast, higher compensation destroys the natural damping of the machine [2].

### 1.3 Objectives

The objective of this work is to develop a reliable PSS tuning method that operates on the mode damping directly to achieve the maximum damping for the un-damped oscillatory modes to enhance the overall small signal stability of the system

### 1.4 Study Outline

- Chapter Two: shows literature review on the Power System Stabilizer tuning approaches along with their advantages and disadvantages.
- Chapter Three: provides an insight into the theory behind the new tuning method, mathematical formulation of the proposed method and a detailed explanation of the method implementation.
- Chapter Four: presents the results of the algorithm and the simulation outcomes when applying these results on the two-area four-machine system and the IEEE9-Bus system. Furthermore, it compares between proposed method and other methods used to tune PSS parameters.
- Chapter Five: concludes this work.

# CHAPTER 2

# LITERATURE REVIEW

## 2.1 Tuning Approaches of PSS Parameters

A number of approaches have been used to tune the power system stabilizer. Some methods involve using pole placement techniques such as the residue-based method. It defines the open loop transfer function of the system between two points; reference voltage as the $i^{th}$ input (generator excitation input) and rotation speed as the $j^{th}$ output. That is:

$$P_{ij}(s) = \sum_{h=1}^{n} \frac{r_{ij}^{h}}{s - \lambda_h} \tag{2.1}$$

Where n is the total number of the eigenvalues and $\lambda_h$ is the $h^{th}$ eigenvalue. $r^h_{ij}$ is the residue of $P_{ij}$ for the $h^{th}$ eigenvalue. As, assume the power system stabilizer has a transfer function of the following form:

$$M(s) = K_e G(s) \tag{2.2}$$

Then the phase shift of the $h^{th}$ eigenvalue will be:

$$\Delta\lambda_h = r_{ij}^{h}.\Delta M(\lambda_h) \approx r_{ij}^{h}.G(\lambda_h).\Delta K_e \tag{2.3}$$

Based on equation (2.3), if:

$$\angle r_{ij}^{h} + \angle G(\lambda_h) = \pm 180 \tag{2.4}$$

Then, a negative value for ΔKe is satisfactory to shift the $h^{th}$ eigenvalue ($\lambda_h$) to the left side of the complex plane.

However, as represented by [3] the residue-based method does not provide any information about the PSS gain. Furthermore, it is difficult to find parameters for G(s) that offer the required phase shift over a wide range of frequencies.

In a different approach, de Mello and Concordia described the transfer function between the reference voltage and the output electrical torque as the generator, excitation system and power system transfer function (GEP(s)) [3].The GEP function is extracted by conducting a frequency response measurement between the terminal generator voltage and the reference voltage input to exciter.

$$GEP(j\omega) = \frac{V_t(j\omega)}{V_{ref}(j\omega)} \tag{2.5}$$

The justification for using (j$\omega$) only is that the modes of concern are lightly damped.

A robust power system stabilizer should provide the required phase compensation for this transfer function over the frequencies of concern. The gain can be determined experimentally as one third of the gain value that leads to the system instability.

A third approach for a multi-machine system [3] defines the P-Vr transfer function as the transfer function between the voltage reference and the electrical power when the dynamics of all other machines are disabled. Disabling dynamics by setting $\Delta\delta=0$ is only possible in a simulated environment. The power system stabilizer transfer function ($G_j(j\omega)$) should compensate for the magnitude and phase shift produced by P-$V_r$ transfer function ($H_{Pjj}(j\omega)$) for machine j, Hence:

$$G_j(j\omega) = \frac{1}{H_{PJJ}(j\omega)} \tag{2.6}$$

In order to introduce left shift for the mode $\lambda_h$, the compensation angle should be:

$$\arg\{G_j(j\omega)\} = -\arg\{H_{PJJ}(j\omega)\} \tag{2.7}$$

Designing a PSS based on these equations is relatively simple since $H_{Pjj}(j\omega)$ is a straightforward transfer function containing no interaction dynamics from other generators.

Other tuning algorithms count on the eigenvalue sensitivity approach. The eigenvalue ($\lambda_i$) can be shifted by controlling the PSS parameters denoted by q. Consider the equation from [4]:

$$\frac{\partial \lambda_i}{\partial q} = \frac{\Psi_{ia}^T \frac{\partial A_a}{\partial q} \phi_{ia}}{\Psi_i^T \phi_i} \tag{2.8}$$

Where $A_a$ is the state matrix, $\Psi_i$ and $\phi_i$ are the left and right eigenvectors associated with $\lambda_i$ and

$$\Psi_{ia} = [\Psi_i^T \quad \Psi_{iv}^T]^T \ , \quad \phi_{ia} = [\phi_i^T \quad \phi_{iv}^T]^T$$

The above expression provides an estimate of the mode shift when PSS parameter (q) is changed. Small Signal Stability Analysis Package (SSAP) was used in [4] to investigate the eigenvalue analysis of the China Southern Power Grid (CSG). Some PSS parameters have been adjusted and results show an improvement in the system stability. However, a change in PSS parameters can cause conflicting effect on different modes.

The challenge becomes to shift $\lambda_i$ to the left by changing the real part while keeping the imaginary part unchanged.

In [5], a modal decomposition method to reduce the interaction between different modes was proposed. It aims to dampen a particular inter-area mode without affecting other modes; this makes the tuning problem much easier. However, this proposed PSS cannot stand-alone. Basically, it helps the conventional PSS to improve the damping of particular inter-area modes.

This modal interaction is mentioned in [6]. It shows that a mode in any area can be excited by a mode in another area due to resonance. Furthermore, it relates between the effectiveness of the PSS and load voltage characteristics. For inter-area modes, it finds that the effectiveness of the

PSS with constant power load is lower than its effectiveness when using constant impedance load model.

### 2.2 Overview of Different PSS Structures

Depending on the stabilizing signal, Power System Stabilizers have various structures. Rotor speed, integral of power and frequency are the most commonly used input signals.

1. Stabilizer based on rotor speed signal (Delta-Omega)

This simple structure uses the rotational speed measured from the shaft as an input signal to the stabilizer. An example of such stabilizer is the one proposed by [7] and shown in figure (2.1)

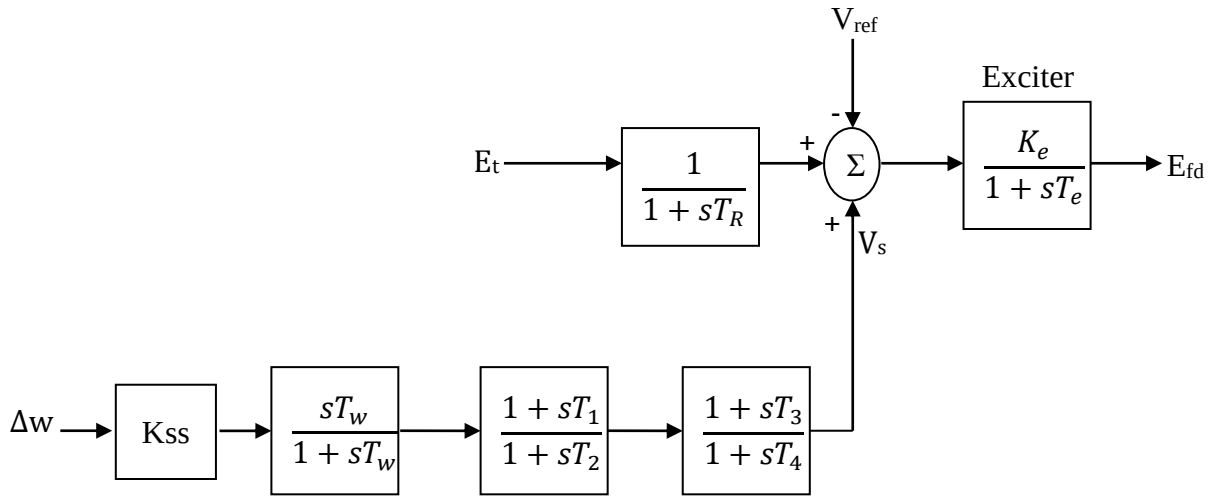


Figure 2.1 Excitation System with PSS

The main concern of Delta-Omega stabilizer is that the shaft run-out may distort the input signal (w). Moreover, using sensed rotor speed as an input may affect the stability of torsional modes in thermal units. Torsional filters should be used to solve this problem.

To tune the parameters of Delta-Omega stabilizer, the first step is to compute the open loop frequency response between the exciter input and the electrical torque using a software program such as MASS. Designed PSS should compensate for the resulting frequency response. The stabilizer gain should be selected as the value that leads to maximum damping. The torsional filter may limit this value.

2. Delta-P-Omega stabilizer

Since the rotor speed and the power have a direct relationship, Delta-P-Omega stabilizer was developed to master the limitations of the Delta-Omega stabilizer. The measurement of accelerating power does not contain torsional modes thus there is no need for torsional filter. Additionally, it allows for higher gain that leads to higher oscillations damping.

According to the swing equation:

$$\frac{d\,\Delta\omega_r}{dt} = \frac{1}{2H}(P_m - P_e) \tag{2.9}$$

Practically, mechanical power can be taken as a constant and the electrical power becomes directly proportional to the rotor speed. This assumption turns out to be invalid in the cases of load changing.

3. Frequency based stabilizer

System frequency can also be used as a stabilizing signal. This type of stabilizers offers better damping for inter-area low frequency oscillations while it has less sensitivity to the local modes.

Its main disadvantage appears in rapid transients where the frequency experience sudden phase shift giving incorrect results. Moreover, torsional filters are necessary to attenuate torsional mode.

4. Multi-Band stabilizer (MB-PSS)

The main reason behind developing the MB-PSS is to cover a wide range of oscillation frequencies. Systems with long tie lines may suffer from inter-area mode with very low frequencies (0.2 Hz) and local modes with as high as 4 Hz. Conventional Delta-Omega stabilizer cannot work efficiently to damp all these modes.

As [8], MB-PSS categorizes the electromechanical oscillation into three categories named low, intermediate and high frequency modes of oscillation. Accordingly, it consists of three working bands as seen in figure (2.2). Each band involves a gain, differential bandpass filter, limiter and phase compensator.

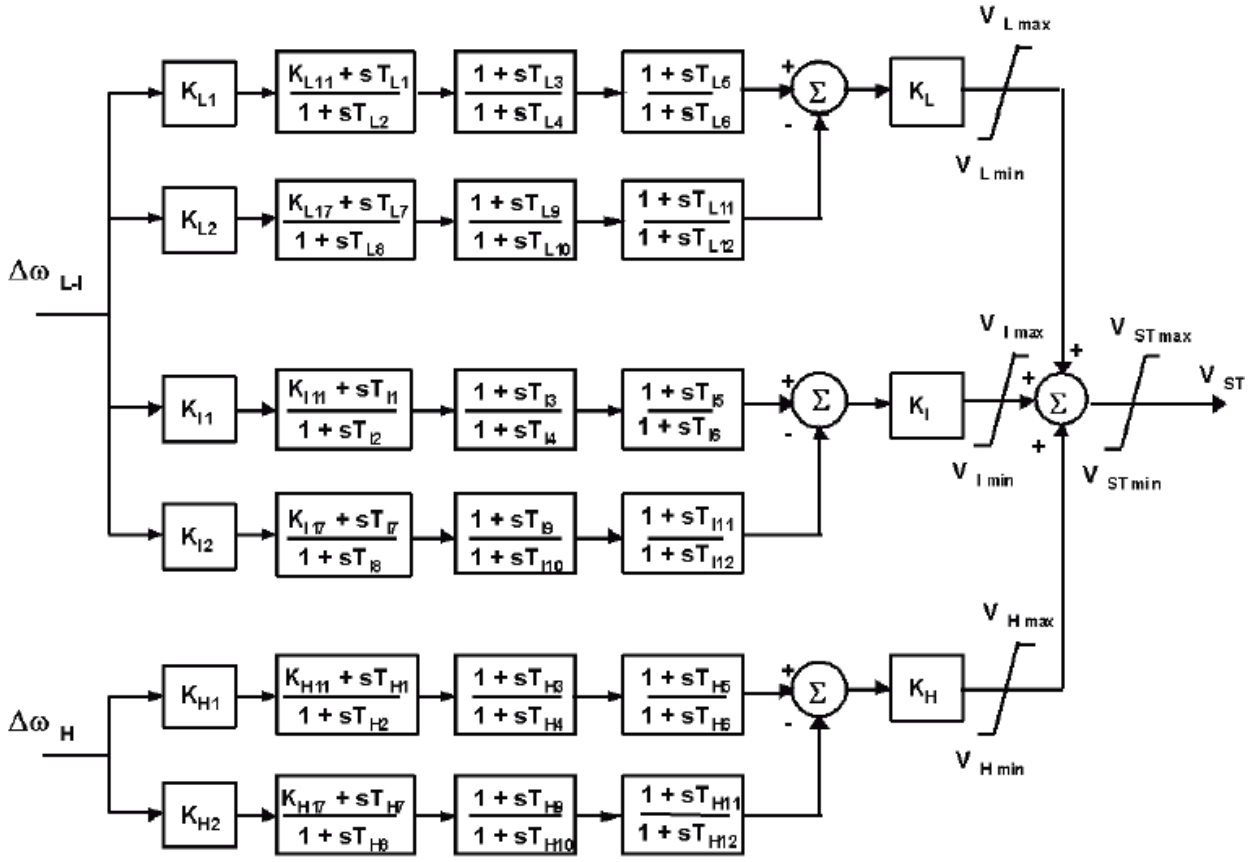


Figure 2.2 Multi-Band PSS

Low frequency band works in the range of (<0.2 Hz) while the intermediate frequency band takes care of the frequencies between 0.2 Hz and 1.0 Hz. High frequency band is associated with higher frequencies such as (0.8-4 Hz).

MB-PSS uses two speed deviation transducers to create two different inputs. Figure (2.3) shows the speed deviation transducers and a bank of two tunable notch filters to filter the high frequency torsional modes.

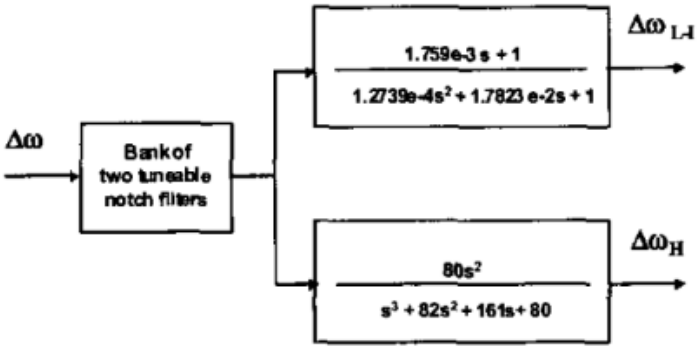


Figure 2.3 Speed Deviation Transducers

To tune the MB-PSS, [8] presented simple equations to solve for six variable for each band; central frequencies $F_L$, $F_I$, $F_H$ and gains $K_L$, $K_I$, $K_H$. Consider the high frequency band shown in figure (2.4) as an example, then:

$$K_{H11} = K_{H17} = 1 \tag{2.10}$$

$$T_{H2} = T_{H7} = \frac{1}{2\pi F_H \sqrt{R}} \tag{2.11}$$

$$T_{H1} = \frac{T_{H2}}{R} \tag{2.12}$$

$$T_{H8} = T_{H7} \times R \tag{2.13}$$

$$K_{H1} = K_{H2} = \frac{R^2 + R}{R^2 - 2R + 1} \tag{2.14}$$

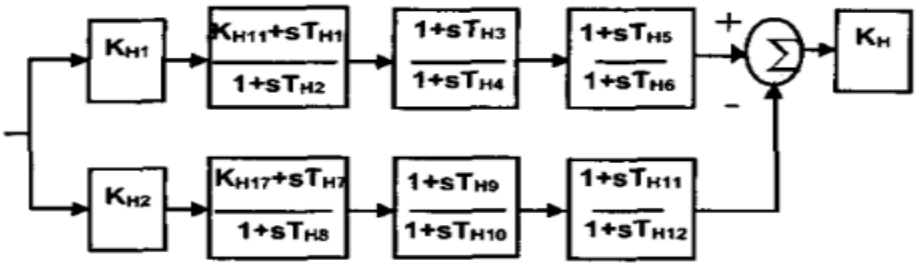


Figure 2.4 The High Band Differential Filter

# CHAPTER 3

# METHODOLOGY

## 3.1 Introduction

A power System Stabilizer is a device that operates on the exciter voltage to damp the rotor oscillations produced by small disturbances. Its basic function is to extend the angular stability limits of the power system by generating a component of electrical torque in phase with the rotor speed deviation. To achieve this goal, it feeds back a stabilizing signal (speed deviation or electrical power) to the excitation system through lead-phase compensation blocks. The lead phase blocks compensate for the lag-phase generated by the generator and excitation system. The good functionality of the power system stabilizer is measured by its ability to provide the required gain/phase compensation. Thus, designing the phase compensation blocks has very important role in improving the power system stability.

This work presents a new method to tune parameters of the power system stabilizer aiming to achieve the maximum damping for the undamped oscillatory modes. It uses the power system stabilizer model defined in Kundur [7], which consists of a gain and two phase-lead compensation blocks.

The new concept utilizes a small signal stability approach to formulate an explicit expression for the damping sensitivity with respect to the power system stabilizer parameters. Through an iterative procedure, it calculates the correct time constant values (T1, T2, T3, T4 and

Kss) of the lead-phase compensation blocks. Calculated parameters are then applied to provide the maximum damping by providing the most suitable phase compensation.

The next section reviews the background of the small signal stability theory. Section 3.2 explains the novel concept for damping sensitivity calculation. Application of the proposed concept on the single machine infinite bus system is presented in section 3.3. Proposed procedure to tune the power system stabilizer presented in section 3.4.

## 3.2 Background

### *3.2.1 State Space Representation*

Dynamic systems such as power systems can be represented by a set of n nonlinear differential equations as follows:

$$\dot{x}_i = f_i(x_1, x_2, \dots, x_n; u_1, u_2, \dots, u_r; t) \qquad \text{i=1, 2, ..., n} \tag{3.1}$$

Where n is the order of the system, r is the number of inputs and t is the time.

Equation (3.1) can be stated in matrices form using state vector (x) and input vector (u) as:

$$\dot{x} = f(x, u, t) \tag{3.2}$$

Where:

$$x = \begin{bmatrix} x_1 \\ \vdots \\ x_n \end{bmatrix} \qquad u = \begin{bmatrix} u_1 \\ \vdots \\ u_r \end{bmatrix}$$

State vector (x) consists of n state variables which are defined as the minimum number of variables at time $t_0$ that are required to characterize the behavior of the system in the future. On the other hand, input vector (u) contains the r external input signals.

If the differential functions in equation (3.2) are not direct time dependent functions, the system is called autonomous and defined as below:

$$\dot{x} = f(x, u) \tag{3.3}$$

In a like way, the m output variables vector (y) can be defined as:

$$y = g(x, u) \tag{3.4}$$

### *3.2.2 Equilibrium Points*

These are the points where all the n first order differential equations are simultaneously equal to zero. In other words, equilibrium points are the points were all the system variables are at rest with respect to time. Mathematically, equilibrium points should satisfy the equation:

$$f(x_0) = 0 \tag{3.5}$$

A dynamic system is said to be stable about an equilibrium points if, after small disturbance, it converges to (or nearby) the equilibrium points.

### *3.2.3 Linearization*

To linearize equation (3.3) around the equilibrium point after small perturbation, it may be expressed as:

$$\begin{aligned} \dot{x} &= \dot{x}_0 + \Delta\dot{x} \\ &= f[(x_0 + \Delta x), (u_0 + \Delta u)] \end{aligned} \tag{3.6}$$

Where:

$$\dot{x}_0 = f(x_0, u_0) \tag{3.7}$$

$x_0$ is the initial state vector and $u_0$ is the input vector corresponding to the equilibrium point.

The above equation can be solved using Taylor's series expansion with second and higher order terms neglected

$$\dot{x}_i = \dot{x}_{i0} + \Delta\dot{x}_i = f_i[(x_0 + \Delta x), (u_0 + \Delta u)]$$

$$= f_i(x_0 + u_0) + \frac{\partial f_i}{\partial x_1}\Delta x_1 + \cdots + \frac{\partial f_i}{\partial x_n}\Delta x_n + \frac{\partial f_i}{\partial u_1}\Delta u_1 + \cdots + \frac{\partial f_i}{\partial u_n}\Delta u_n \tag{3.8}$$

By comparing equation (3.7) and equation (3.8), the expression of the change in the derivative of the state variable $\Delta\dot{x}_i$ can be obtained as:

$$\Delta\dot{x}_i = \frac{\partial f_i}{\partial x_1}\Delta x_1 + \cdots + \frac{\partial f_i}{\partial x_n}\Delta x_n + \frac{\partial f_i}{\partial u_1}\Delta u_1 + \cdots + \frac{\partial f_i}{\partial u_r}\Delta u_r \tag{3.9}$$

And the change in output is:

$$\Delta y_i = \frac{\partial g_j}{\partial x_1}\Delta x_1 + \cdots + \frac{\partial g_j}{\partial x_n}\Delta x_n + \frac{\partial g_j}{\partial u_1}\Delta u_1 + \cdots + \frac{\partial g_j}{\partial u_r}\Delta u_r \tag{3.10}$$

Equations (3.9) & (3.10) can be rewritten as:

$$\Delta\dot{x} = A\Delta x + B\Delta u \tag{3.11}$$

$$\Delta y = C\Delta x + D\Delta u \tag{3.12}$$

Where:

$$A = \begin{bmatrix} \frac{\partial f_1}{\partial x_1} & \cdots & \frac{\partial f_1}{\partial x_n} \\ \vdots & \ddots & \vdots \\ \frac{\partial f_n}{\partial x_1} & \cdots & \frac{\partial f_n}{\partial x_n} \end{bmatrix} \qquad B = \begin{bmatrix} \frac{\partial f_1}{\partial u_1} & \cdots & \frac{\partial f_1}{\partial u_r} \\ \vdots & \ddots & \vdots \\ \frac{\partial f_n}{\partial u_1} & \cdots & \frac{\partial f_n}{\partial u_r} \end{bmatrix}$$

$$C = \begin{bmatrix} \frac{\partial g_1}{\partial x_1} & \cdots & \frac{\partial g_1}{\partial x_n} \\ \vdots & \ddots & \vdots \\ \frac{\partial g_m}{\partial x_1} & \cdots & \frac{\partial g_m}{\partial x_n} \end{bmatrix} \qquad D = \begin{bmatrix} \frac{\partial g_1}{\partial u_1} & \cdots & \frac{\partial g_1}{\partial u_r} \\ \vdots & \ddots & \vdots \\ \frac{\partial g_m}{\partial u_1} & \cdots & \frac{\partial g_m}{\partial u_r} \end{bmatrix}$$

The above equation can be expressed in the frequency domain as following:

$$s\Delta x(s) - \Delta x(0) = A\Delta x(s) + B\Delta u(s) \tag{3.13}$$

$$\Delta y(s) = C\Delta x(s) + D\Delta u(s) \tag{3.14}$$

They can also be represented as the block diagram shown in figure (3.1) assuming the initial conditions are zero.

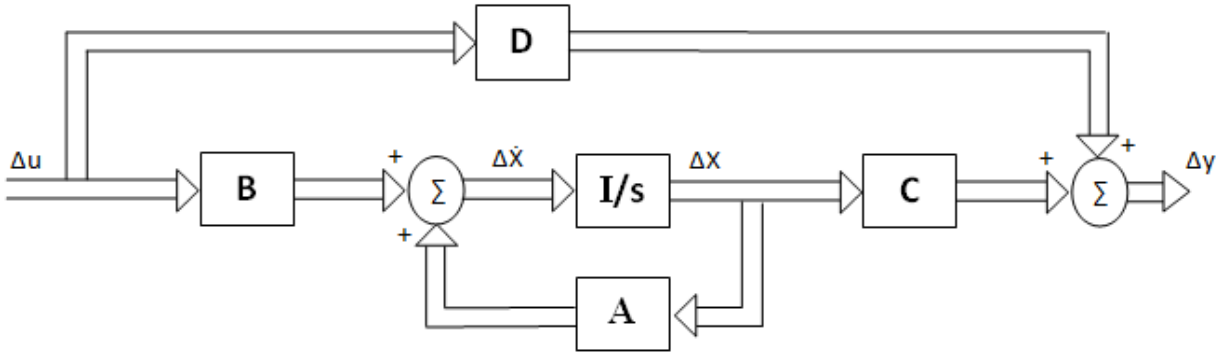


Figure 3.1 Block Diagram of the State Space Representation

Solving for Δx(s):

$$(sI - A)\Delta x(s) = \Delta x(0) + B\Delta u(s) \tag{3.15}$$

Then

$$\Delta x(s) = (sI - A)^{-1}[\Delta x(0) + B\Delta u(s)] \tag{3.16}$$

$$= \frac{adj(sI - A)}{\det(sI - A)}[\Delta x(0) + B\Delta u(s)] \tag{3.17}$$

And

$$\Delta y(s) = C\frac{adj(sI-A)}{\det(sI-A)}[\Delta x(0) + B\Delta u(s)] + D\Delta u(s) \tag{3.18}$$

The poles of Δx and Δy are called the eigenvalues of matrix A and can be found by solving for the roots of the characteristic equation:

$$\det(sI - A) = 0 \tag{3.19}$$

### *3.2.4 Eigenvalues*

As [7], eigenvalues are the values of the scalar parameter λ for which there exist non-trivial solution to the equation:

$$A\phi = \lambda\phi \tag{3.20}$$

Where A is an nxn matrix and ϕ is an nx1 vector.

Rearranging equation (3.20):

$$(A - \lambda I)\phi = 0 \tag{3.21}$$

Now solve:

$$det(A - \lambda I) = 0 \tag{3.22}$$

The n solutions of above equation are the eigenvalues of the state matrix A.

### *3.2.5 Eigenvectors*

From equation (3.20), the resulting column vector $\phi_i$ when $\lambda=\lambda_i$ is called the right eigenvector of A associated with eigenvalue $\lambda_i$, that is:

$$A\phi_i = \lambda_i\phi_i \tag{3.23}$$

$\phi_i$ has the form:

$$\phi_i = \begin{bmatrix} \phi_{1i} \\ \phi_{2i} \\ \vdots \\ \phi_{ni} \end{bmatrix} \tag{3.24}$$

The left eigenvector Ψi associated with eigenvalue $\lambda_i$ is the row vector which fulfils the equation:

$$\Psi_i A = \lambda_i \Psi_i \tag{3.25}$$

Where:

$$\Psi_i = [\Psi_{1i} \quad \Psi_{2i} \quad ... \quad \Psi_{ni}] \tag{3.26}$$

The left eigenvectors and right eigenvectors associated with different eigenvalues are orthogonal. Hence:

$$\Psi_j \phi_i = 0 \tag{3.27}$$

On the other hand:

$$\Psi_i \phi_i = C_i \tag{3.28}$$

Where $C_i$ is a non-zero constant. Equation (3.28) can be normalized such that:

$$\Psi_i \phi_i = 1 \tag{3.29}$$

This can be expanded as:

$$\Psi \phi = 1$$

Then:

$$\Psi = \phi^{-1} \tag{3.30}$$

### *3.2.6 Modal Matrices*

Define the following matrices:

$$\phi = [\phi_1 \quad \phi_2 \quad ... \quad \phi_n] \tag{3.31}$$

$$\Psi = [\Psi_1^T \quad \Psi_2^T \quad ... \quad \Psi_n^T]^T \tag{3.32}$$

$\Lambda$ = diagonal matrix where the diagonal values are the eigenvalues. (3.33)

Using these matrices, equation (3.23) can be rewritten as:

$$A\phi = \phi\Lambda \tag{3.34}$$

Substituting in equation (3.33):

$$\phi^{-1}A\phi = \Lambda \tag{3.35}$$

### *3.2.7 Free Motion of a Dynamic System*

Equation (3.11) comprises two components named free and zero state. Considering only the free component:

$$\Delta\dot{x} = A\Delta x \tag{3.36}$$

These are the equations that physically describe the behavior of the system with zero input. For real systems, each one of these derivatives is a function of all the state variables. To remove the cross-coupling between the state variables, define a new state vector z as following:

$$\Delta x = \phi z \tag{3.37}$$

Substitute the new value of Δx in (3.36):

$$\phi\dot{z} = A\phi z \tag{3.38}$$

Yields:

$$\dot{z} = \phi^{-1}A\phi z \tag{3.39}$$

Or:

$$\dot{z} = \Lambda z \tag{3.40}$$

Since Λ is a diagonal matrix, equation (3. 40) defines n uncoupled first order equations in the form:

$$\dot{z}_i = \lambda_i z_i \tag{3.41}$$

The solution for this equation with respect to time is:

$$z_i(t) = z_i(0)e^{\lambda_i t} \tag{3.42}$$

$z_i(0)$ is the initial value of $z_i$. The solution expression referred to the original state vector is given by:

$$\Delta x(t) = \phi z(t) \tag{3.43}$$

$$= [\phi_1 \quad \phi_2 \quad \dots \quad \phi_n] \begin{bmatrix} z_1(t) \\ z_2(t) \\ \vdots \\ z_n(t) \end{bmatrix} \tag{3.44}$$

Or:

$$\Delta x(t) = \sum_{i=1}^{n} \phi_i z_i(0) e^{\lambda_i t} \tag{3.45}$$

The expression of z(t) from equation (3.43) is:

$$z(t) = \phi^{-1} \Delta x(t) = \Psi \Delta x(t) \tag{3.46}$$

For specific state variable j:

$$z_j(t) = \Psi_j \Delta x(t) \tag{3.47}$$

When t=0:

$$z_j(0) = \Psi_j \Delta x(0) \tag{3.48}$$

Substitute in equation (3.45) with replacing the scalar product $\Psi_j \Delta x(0)$ by $c_j$:

$$\Delta x(t) = \sum_{j=1}^{n} \phi_j c_j e^{\lambda_j t} \tag{3.49}$$

Equation (3.49) can be expanded as follows:

$$\Delta x_j(t) = \phi_{j1} c_1 e^{\lambda_1 t} + \phi_{j2} c_2 e^{\lambda_2 t} + \cdots + \phi_{jn} c_n e^{\lambda_n t} \tag{3.50}$$

Equation (3.50) represents the free motion time response corresponding to the $j^{th}$ state variable. In each term, the scalar product $c_j$ denotes the magnitude of the excitation of the particular eigenvalue (or mode). The time dependent characteristic of the mode is defined by the value of $e^{\lambda_j t}$. Consequently, the eigenvalues can be used to investigate the stability of the system. Real

eigenvalues represents non oscillatory modes. They are either decaying modes in case of the negative real eigenvalues or aperiodic unstable modes if they have positive sign. However, complex eigenvalues occur in conjugate pairs and indicate to oscillatory mode behavior such that:

$$\lambda = \sigma \pm j\omega \tag{3.51}$$

The oscillation frequency in Hz is:

$$f = \frac{\omega}{2\pi} \tag{3.52}$$

Using eigenvalues, the damping ratio can be calculated for each eigenvalue (mode) as follows:

$$\zeta = \frac{-\sigma}{\sqrt{(\sigma^2+\omega^2)}} \tag{3.53}$$

### *3.2.8 Eigenvalue Sensitivity*

Eigenvalue sensitivity states the most effective state variables in a particular mode among other state variables. It can be calculated by differentiating the eigenvalue of interest with respect to state matrix entries. Start with equation (3.23):

$$A\phi_i = \lambda_i \phi_i$$

Taking the derivative with respect to $a_{kj}$ (the element in $k^{th}$ row and $j^{th}$ column) as:

$$\frac{\partial A}{\partial a_{kj}}\phi_i + A\frac{\partial \phi_i}{\partial a_{kj}} = \frac{\partial \lambda_i}{\partial a_{kj}}\phi_i + \lambda_i \frac{\partial \phi_i}{\partial a_{kj}} \tag{3.54}$$

Multiplying equation (3.54) by $\Psi_i$ with considering $\Psi_i \phi_i=1$ and $\Psi_i(A- \lambda_i I)=0$ yields:

$$\Psi i \frac{\partial A}{\partial a_{kj}}\phi_i = \frac{\partial \lambda_i}{\partial a_{kj}} \tag{3.55}$$

The partial differentiation of any element in state matrix A with respect to another element is always zero except for the case of differentiating the element with respect to itself which gives 1. Hence,

$$\frac{\partial \lambda_i}{\partial a_{kj}} = \Psi_{ik}\phi_{ji} \tag{3.56}$$

### *3.2.9 Participation Factor*

To eliminate the scaling dependency associated with the right and left eigenvectors, a matrix called participation matrix (P) may be defined as:

$$P = [P_1 \quad P_2 \quad \dots \quad P_n] \tag{3.57}$$

Where:

$$p_i = \begin{bmatrix} p_{1i} \\ p_{2i} \\ \vdots \\ p_{ni} \end{bmatrix} = \begin{bmatrix} \Psi_{1i}\phi_{i1} \\ \Psi_{2i}\phi_{i2} \\ \vdots \\ \Psi_{ni}\phi_{in} \end{bmatrix} \tag{3.58}$$

$\phi_{ki}$ is the $k^{th}$ entry of the right eigenvector $\phi_i$ while $\Psi_{ik}$ is the $k^{th}$ entry of the left eigenvector $\Psi_i$. The product $\phi_{ki}\,\Psi_{ik}$ is a measure of the participation of $k^{th}$ state variable in the $i^{th}$ mode.

## 3.3 Novel Concept for Damping Sensitivity Calculation

Equation (2.56) presents the sensitivity of mode (i) with respect to element $a_{kj}$ of the state matrix A. A general Mode Sensitivity Matrix (MSM) for mode k can be defined as follows:

$$(MSM^k) = \begin{bmatrix} \Psi_{k1}.\phi_{1k} & \cdots & \Psi_{kn}.\phi_{1k} \\ \vdots & \ddots & \vdots \\ \Psi_{k1}.\phi_{nk} & \cdots & \Psi_{kn}.\phi_{nk} \end{bmatrix} \tag{3.59}$$

$(MSM)^k$ defines the sensitivity of the $K^{th}$ mode( $\frac{\partial \lambda_i}{\partial a_{ij}}$) w ith respect to all elements $a_{ij}$ of the state matrix.

Since $\lambda_k=\sigma_k+j\omega_k$, then:

$$(MSM^k)_{real} = \begin{bmatrix} \frac{\partial \sigma_k}{\partial a_{11}} & \cdots & \frac{\partial \sigma_k}{\partial a_{1n}} \\ \vdots & \ddots & \vdots \\ \frac{\partial \sigma_k}{\partial a_{n1}} & \cdots & \frac{\partial \sigma_k}{\partial a_{nn}} \end{bmatrix} \qquad (MSM^k)_{imag} = \begin{bmatrix} \frac{\partial \omega_k}{\partial a_{11}} & \cdots & \frac{\partial \omega_k}{\partial a_{1n}} \\ \vdots & \ddots & \vdots \\ \frac{\partial \omega_k}{\partial a_{n1}} & \cdots & \frac{\partial \omega_k}{\partial a_{nn}} \end{bmatrix} \tag{3.60}$$

Considering the damping ratio $\zeta$ defined by equation (3.53); its derivative with respect to the state matrix elements is easily obtained as:

$$\frac{\partial \zeta_k}{\partial a_{ij}} = \frac{-\omega_k}{(\sigma_k^2 + \omega_k^2)^{\frac{3}{2}}} \cdot \left( \omega_k \frac{\partial \sigma_k}{\partial a_{ij}} - \sigma_k \frac{\partial \omega_k}{\partial a_{ij}} \right) \tag{3.61}$$

In matrix form and with reference to equation (3.60), this may be extended to all elements of the state matrix as follows:

$$\frac{\partial \zeta_k}{\partial A} = \frac{-\omega_k}{(\sigma_k^2 + \omega_k^2)^{\frac{3}{2}}} \cdot \left( \omega_k (MSM^k)_{real} - \sigma_k (MSM^k)_{imag} \right) \tag{3.62}$$

The resulting matrix may be called the Damping Sensitivity Matrix for mode k, $DSM^k$

### 3.4 Single Machine Infinite Bus System

To demonstrate the new method for damping sensitivity calculation and its effectiveness in improving the system stability by providing the required phase-lead compensation, it has been applied to the single machine infinite bus system mentioned in Kundur example 12.3 [7] shown in figure (3.2).

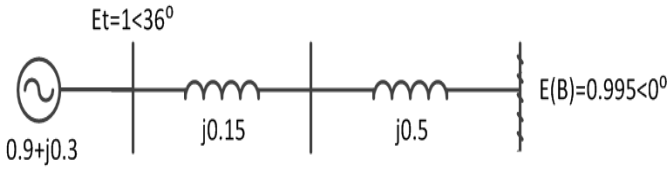


Figure 3.2 Single Machine Infinite Bus System

#### *3.4.1 Synchronous Machine Model*

To analyze the systems stability, it is a common practice to use a simplified model of the synchronous machine. The first order of simplification is to neglect the stator transients and the effect of speed variation on power. By ignoring the stator transients, only the fundamental frequency components of stator quantities will be considered which allows the use of steady state relationships to represent the transmission network and consequently reduces the problem's dimension. Neglecting effect of speed variation makes the pu power and torque interchangeable. Two sets of equations were used to form the small signal model of the synchronous machine:

1. State variables

Four state variables were used to describe the synchronous machine and build the system state matrix

a. Voltage behind transient reactance($X'_d$) equation

This voltage was represented by the following equation:

$$pE'_q = \frac{1}{T'_{d0}}[-E'_q - (X_d - X'_d)i_d] \tag{3.63}$$

Where $E'_q$ is the q-axis component of the voltage behind transient reactance $X'_d$

$T'_{d0}$ is the open circuit transient time constant

$E_{fd}$ is the field circuit voltage

$X_d$ and $X'_d$ are the direct axis reactance and direct axis transient reactance respectively

$I_d$ is the direct axis current

Using $E'_q$ as state variable allows including the field circuit dynamics which are important for dynamic analysis.

The small signal form of equation (3.63) is:

$$\Delta\dot{E}'_q = \frac{1}{T_{d0}}[\Delta E_{fd} - \Delta E'_q - (X_d - X'_d).\Delta I_d] \tag{3.64}$$

b. Field voltage equation

The simple exciter model shown in figure (3.3) was used. The following equation expresses the output voltage:

$$\dot{E_{fd}} = \frac{1}{T_e}[(K_e(V_{ref} - V_t) - E_{fd}] \tag{3.65}$$

Where $K_e$, $T_e$ are the exciter gain and time constant respectively.

$V_{ref}$ is the reference voltage

$V_t$ is the synchronous machine terminal voltage

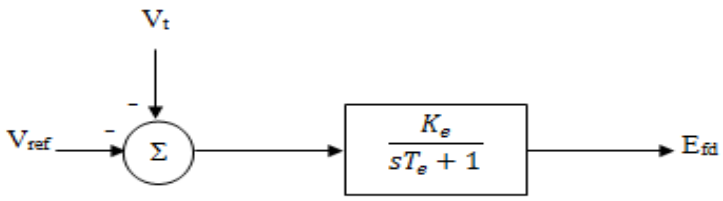


Figure 3.3 Excitation System

For small disturbances the equation becomes:

$$\Delta\dot{E}_{fd} = \frac{1}{T_e}\left(-K_e\Delta V_t - \Delta E_{fd}\right) \tag{3.66}$$

c. Swing equations

Swing equations take account of the rotor speed and rotor angle by describing the difference between the electrical torque, mechanical torque and damping torque of the machine under concern as below:

$$\frac{d\,\omega_r}{dt} = \frac{1}{2H}(T_m - T_e - K_D\Delta\,\omega_r) \tag{3.67}$$

$$\frac{d\,\delta}{dt} = \omega_0\Delta\omega_r \tag{3.68}$$

These equations can be linearized as follows, since the pu torque and power are interchangeable, $P_m$ and $P_e$ may be used in place of $T_m$ and $T_e$:

$$\frac{d\,\Delta\omega_r}{dt} = \frac{1}{2H}(P_m - P_e - K_D\Delta\,\omega_r) \tag{3.69}$$

$$\frac{d\Delta\delta}{dt} = \omega_0\Delta\omega_r \tag{3.70}$$

The block diagram of figure (3.4) represents the swing equations.

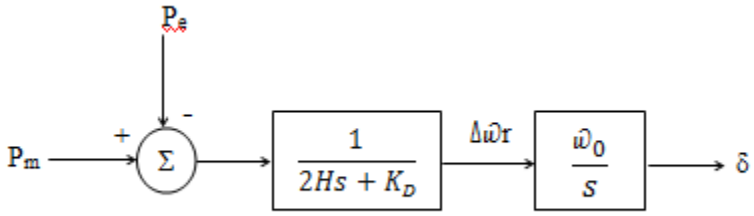


Figure 3.4 Block Diagram Representation of Swing Equations

Equations (3.64), (3.66), (3.69) and (3.70) identify the four state variables of the system.

2. Non state variables

In search of a solution for the state space model defined above, nine additional non-state variables were temporarily used as intermediate variables ($V_t$, $V_d$, $V_q$, $I_d$, $I_q$, $V_x$, $V_y$, $I_x$ and $I_y$) The first three equations were basically derived from the synchronous machine phasor diagram shown in figure (3.5). These three equations are:

$$0 = -\Delta V_d + X_q.\Delta I_q \tag{3.71}$$

$$0 = -\Delta V_q + \Delta E'_q - X'_d.\Delta I_d \tag{3.72}$$

$$0 = -\Delta V_t + \frac{E_q}{V_t}.\Delta V_q + \frac{E_d}{V_t}.\Delta V_d \tag{3.73}$$

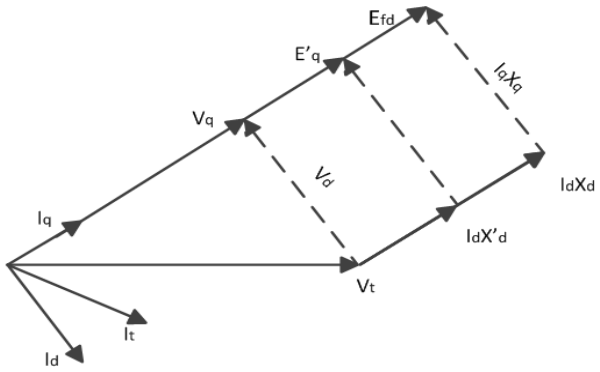


Figure 3.5 Synchronous Machine Phasor Diagram

Figure (3.5) neglects armature resistance $R_a$ due to its small value.

Four equations resulted from the relationship between $E'_q$ in d-q axis and $E'_q$ in the reference axis X-Y as presented in figure (3.6).

$$0 = -\Delta I_d + I_q \Delta\delta + sin\ \delta \Delta I_x - \cos\delta \Delta I_y \tag{3.74}$$

$$0 = -\Delta I_q + I_d \Delta\delta + cos\ \delta \Delta I_x + \sin\delta \Delta I_y \tag{3.75}$$

$$0 = -\Delta V_x - V_y \Delta\delta + sin\ \delta \Delta V_d + \cos\delta \Delta V_q \tag{3.76}$$

$$0 = -\Delta V_y + V_x \Delta\delta + cos\ \delta \Delta V_d + \sin\delta \Delta V_q \tag{3.77}$$

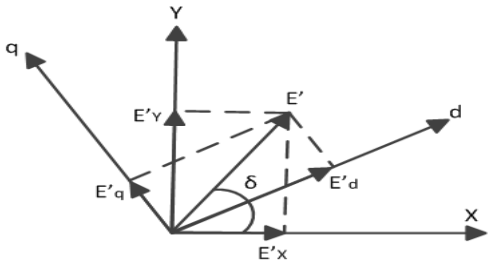


Figure 3.6 Phasor Relationship Between E'q in d-q Axis and E'q in the Reference Axis X-Y

Last two equations are the transmission network equations stated below:

$$0 = -\Delta I_x + \sum_i g_{ij}\Delta V_{xj} - \sum_i b_{ij}\Delta V_{yj} \tag{3.78}$$

$$0 = -\Delta I_y + \sum_i b_{ij}\Delta V_{xj} - \sum_i g_{ij}\Delta V_{yj} \tag{3.79}$$

An ETAP model was built to simulate the synchronous machine and the excitation system behavior. The undamped oscillations experienced by the system after small disturbance are shown in figure (3.7).

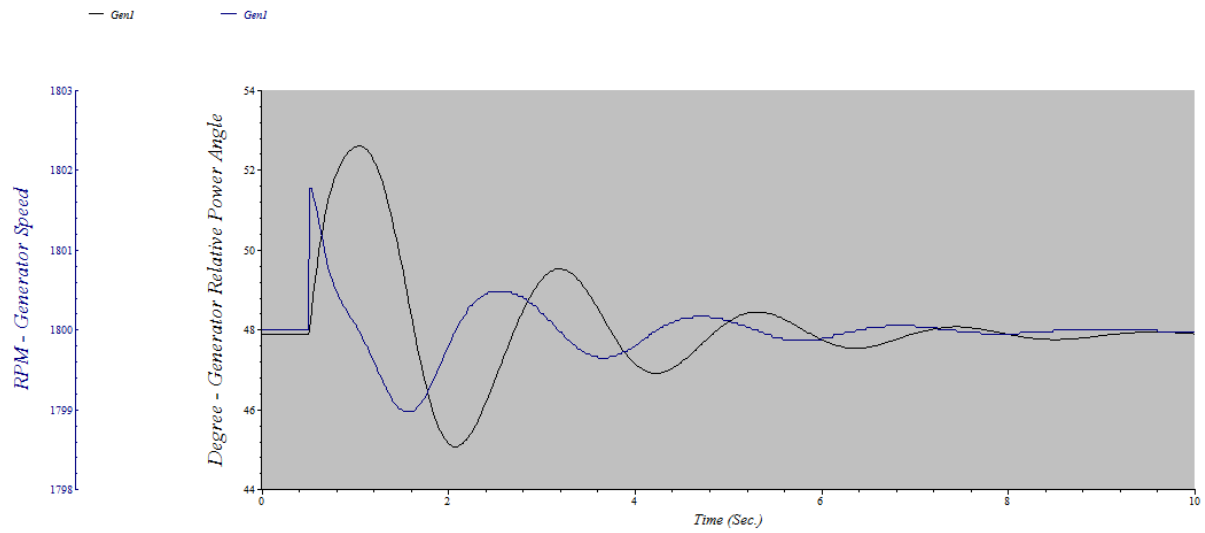


Figure 3.7 Speed and Angle Oscillations

A MATLAB script was also written to find the eigenvalues of the system and the damping ratio for each of them. Table (3.1) presents these eigenvalues and their damping ratios.

Table 3.1 The Eigenvalues and Damping Ratios of the System Before Applying the PSS

| Eigenvalue | Damping Ratio | Participating States |
|---|---|---|
| -1.1294 + 2.8856i | 0.3645 | $E'_q$, $E_{fd}$ |
| -1.1294 - 2.8856i | 0.3645 | $E'_q$, $E_{fd}$ |
| -0.7481 + 6.1535i | 0.1207 | ω, δ |
| -0.7481 - 6.1535i | 0.1207 | ω, δ |

Above results display one under damped oscillatory mode at frequency 6.1535 rad/sec.

### *3.4.2 Power System Stabilizer (PSS)*

A power System Stabilizer is a device that operates on the exciter voltage to damp the rotor oscillations produced by small disturbances. Its basic function is to extend the angular stability limits of the power system by generating a component of electrical torque in phase with the rotor speed deviation.

The block diagram in figure (3.8) [7] provides a good demonstration about the interconnection between the synchronous machine, exciter, Power System Stabilizer (PSS) and Automatic Voltage Regulator (AVR). The designed power system stabilizer uses the speed deviation as a stabilizing signal. Since the synchronous machine transfer function and the exciter transfer function ($G_{ex}(s)$) both are frequency dependent functions, the PSS transfer function ($G_{PSS}(s)$) should be as well.

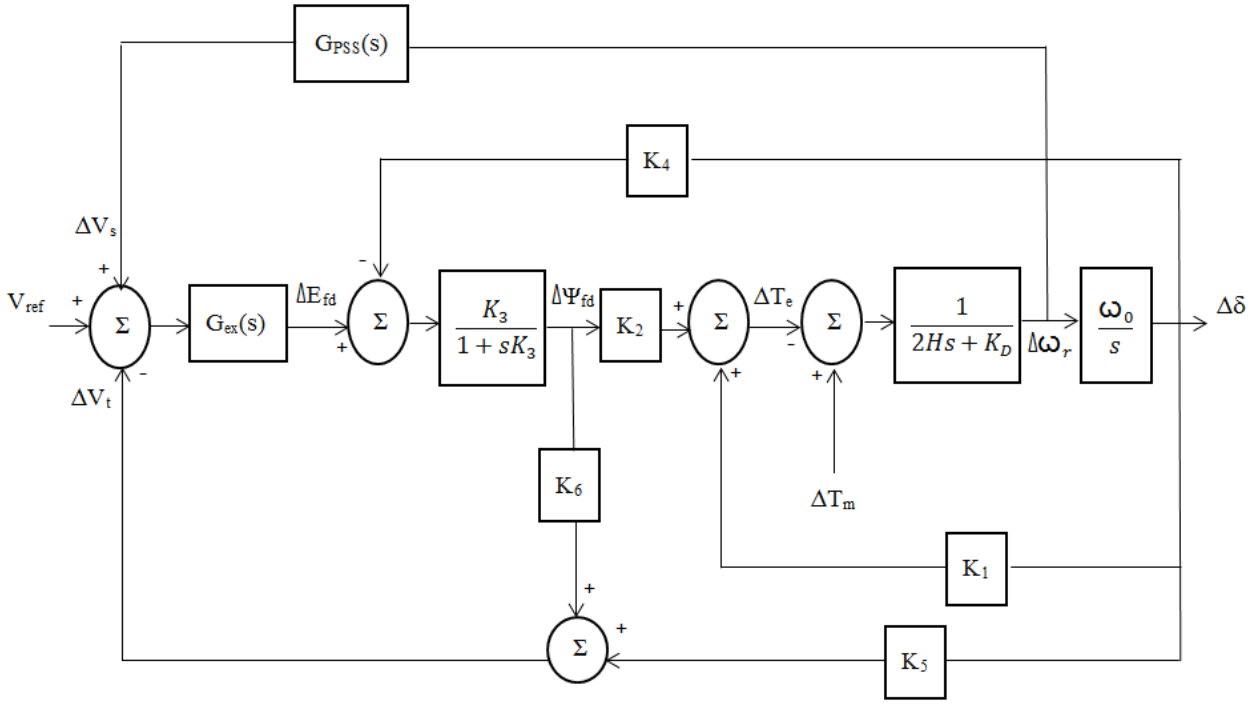


Figure 3.8 Block Diagram Representation with AVR and PSS

The power System stabilizer transfer function should compensate for the phase lag in the generator and exciter transfer functions. The conventional method of designing a PSS is to build a phase-lead circuit which is the inverse of the machine and exciter transfer functions.

### 3.4.2.1 Power System Stabilizer Model

To provide the necessary phase lead compensation, a power system stabilizer of a gain and two phase lead stages was used. The PSS shown in the diagram in figure (3.9) uses the rotor speed as a stabilizing signal. This signal is amplified by the PSS gain and the passes through a washout stage which eliminates the steady state error by blocking DC and low frequency speed

changes and only allowing high frequency speed changes to pass through. The last two blocks of the PSS represent the phase compensation characteristics.

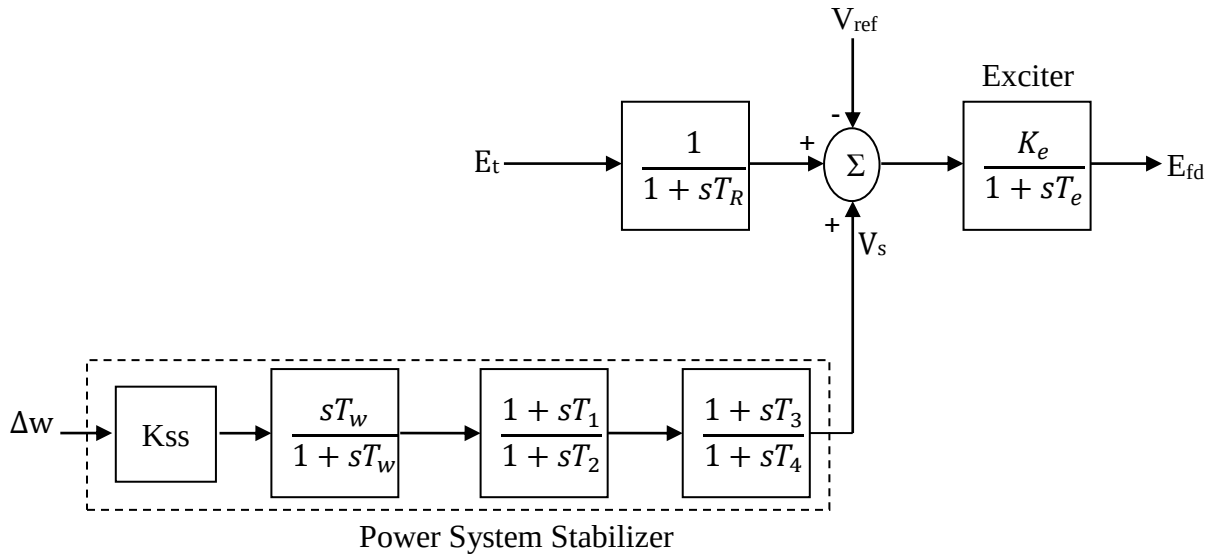


Figure 3.9 Excitation System with PSS

The transfer function of the PSS ignoring the washout filter is:

$$G_{PSS}(s) = Kss \times \frac{1+sT_1}{1+sT_2} \times \frac{1+sT_3}{1+sT_4} \tag{3.80}$$

$$G_{PSS}(s) = Kss \times \frac{1+s(T_1+T_3)+s^2T_1T_3}{1+s(T_2+T_4)+s^2T_2T_4} \tag{3.81}$$

This can be written as:

$$G_{PSS}(s) = Kss \times \frac{1+sTN_1+s^2TN_2}{1+sTD_1+s^2TD_2} \tag{3.82}$$

Where $TN_1=T_1+T_3$, $TN_2=T_1\times T_3$, $TD_1=T_2+T_4$ and $TD_2=T_2\times T_4$

This can be represented by the block diagram in figure (3.10)

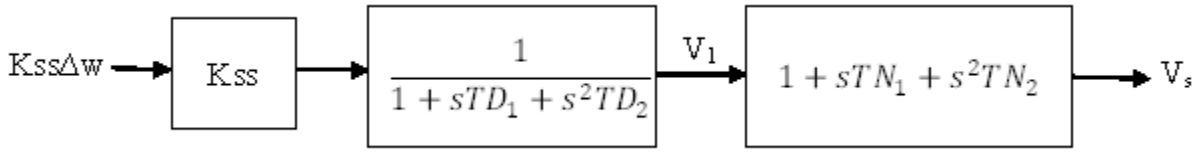


Figure 3.10 Block Diagram Representation of the PSS Transfer Function

The block diagram can be stated in equations form as following, introducing the states $V_1$ and $V_2$:

$$Kss\Delta\omega = V_1 + TD_1 \times sV_1 + TD_2 \times s^2V_1 \tag{3.83}$$

Substituting $sV_1=V_2$:

$$Kss\Delta\omega = V_1 + TD_1 \times V_2 + TD_2 \times sV_2 \tag{3.84}$$

This may be represented in state space format as follows:

$$\begin{bmatrix} sV_1 \\ sV_2 \end{bmatrix} = \begin{bmatrix} 0 & 1 \\ \frac{-1}{TD_2} & \frac{-TD_1}{TD_2} \end{bmatrix} \begin{bmatrix} V_1 \\ V_2 \end{bmatrix} + \begin{bmatrix} 0 \\ \frac{1}{TD_2} \end{bmatrix} Kss\Delta\omega \tag{3.85}$$

The output voltage $V_s$ can be expressed as:

$$\begin{aligned} V_s &= V_1 + TN_1 \times sV_1 + TN_2 \times s^2V_1 \\ &= V_1 + TN_1 \times sV_1 + TN_2 \times sV_2 \end{aligned} \tag{3.86}$$

In matrices form:

$$V_s = V_1 + [TN_1 \;\; TN_2] \begin{bmatrix} sV_1 \\ sV_2 \end{bmatrix} \tag{3.87}$$

$$V_s = V_1 + [TN_1 \;\; TN_2] \begin{bmatrix} 0 & 1 \\ \frac{-1}{TD_2} & \frac{-TD_1}{TD_2} \end{bmatrix} \begin{bmatrix} V_1 \\ V_2 \end{bmatrix} + [TN_1 \;\; TN_2] \begin{bmatrix} 0 \\ \frac{1}{TD_2} \end{bmatrix} Kss\Delta\omega \tag{3.88}$$

### 3.4.2.2 PSS Effect on the State Space Model

Applying the power system stabilizer to the single machine infinite bus system changes its space model by adding two new state variables, $V_1$ and $V_2$ to the state matrix A. These variables are defined in equation (3.85). Furthermore, the power system stabilizer modifies the excitation voltage equation by adding a new term to the differential equation (3.66) as follows:

$$\Delta\dot{E}_{fd} = \frac{1}{T_e}\left(-K_e\Delta V_t - K_e\Delta V_s - \Delta E_{fd}\right) \tag{3.89}$$

Equations (3.85) and (3.88) have feedback components that change the state matrix A by adding six new elements, the first adds three elements to the PSS $V_2$ equation. The other three correspond to the excitation voltage, $E_{fd}$. These elements are shown in table (3.2).

### 3.4.2.3 PSS Tuning

The novel explicit expression for damping sensitivity calculation given by equation (3.62) has facilitated tuning the power system stabilizer parameters. Its strength resides in the fact that it operates on the mode damping directly. It relates the mode damping to the PSS parameters using the state matrix elements.

Section 3.3.2.2 has shown the changes made in the state matrix by applying the PSS. The highlighted state matrix elements shown in table (3.2) are functions of PSS parameters.

Table 3.2 State Matrix A After Applying the PSS

| | $\Delta E'_q$ | $\Delta E_{fd}$ | $\Delta\omega$ | $\Delta\delta$ | $\Delta V_1$ | $\Delta V_2$ |
|---|---|---|---|---|---|---|
| $\Delta E'_q$ | | | | | | |

| | | | | | | |
|---|---|---|---|---|---|---|
| $\Delta E_{fd}$ | | | $\frac{K_e}{T_e}.\frac{TN_2}{TD_2}K_{ss}$ | | $\frac{K_e}{T_e}(1 - \frac{TN_2}{TD_2})$ | $\frac{K_e}{T_e}(TN_1 - \frac{TD_1 TN_2}{TD_2})$ |
| $\Delta\omega$ | | | | | | |
| $\Delta\delta$ | | | | | | |
| $\Delta V_1$ | | | | | | |
| $\Delta V_2$ | | | $\frac{1}{TD_2}K_{ss}$ | | $-\frac{1}{TD_2}$ | $-\frac{TD_1}{TD_2}$ |

Mode damping change can be found as:

$$\Delta\zeta \approx \frac{\partial\zeta}{\partial a_{ij}}\Delta a_{ij} \tag{3.90}$$

For any of the highlighted elements, multi variable calculus gives:

$$\Delta a_{ij} \approx \frac{\partial a_{ij}}{\partial T_1}\Delta T_1 + \frac{\partial a_{ij}}{\partial T_2}\Delta T_2 + \frac{\partial a_{ij}}{\partial T_3}\Delta T_3 + \frac{\partial a_{ij}}{\partial T_4}\Delta T_4 + \frac{\partial a_{ij}}{\partial K_{ss}}\Delta K_{ss} \tag{3.91}$$

Substituting in equation (3.90):

$$\Delta\zeta \approx \frac{\partial\zeta}{\partial a_{ij}}\frac{\partial a_{ij}}{\partial T_1}\Delta T_1 + \frac{\partial\zeta}{\partial a_{ij}}\frac{\partial a_{ij}}{\partial T_2}\Delta T_2 + \frac{\partial\zeta}{\partial a_{ij}}\frac{\partial a_{ij}}{\partial T_3}\Delta T_3 + \frac{\partial\zeta}{\partial a_{ij}}\frac{\partial a_{ij}}{\partial T_4}\Delta T_4 + \frac{\partial\zeta}{\partial a_{ij}}\frac{\partial a_{ij}}{\partial K_{ss}}\Delta K_{ss} \tag{3.92}$$

Each term in equation (3.92) determines the damping sensitivity with respect to one parameter (recall that TN1, TN2, TD1 and TD2 are defined in (3.82)). These sensitivities measure the effect of a predefined change in each parameter on the damping of the specific mode.

MATLAB script was written to examine the effectiveness of the new method on enhancing the damping of the oscillatory modes shown in table (3.1). The initial values of the PSS parameters were set to be:

T1 = 0.05  T2 = 0.02  T3 = 0.05  T4 = 0.02  Kss=0.5

We start with a small change in the gain, ΔKss= 0.5. To calculate $\frac{\partial \zeta}{\partial a_{ij}} \frac{\partial a_{ij}}{\partial K_{ss}} \Delta K_{ss}$, notice that, there are two elements in matrix A that are functions of Kss. Use equation (3.82) to find $\frac{\partial \zeta}{\partial a_{ij}}$ for these two elements corresponding to a particular mode. Then differentiate the two elements with respect to Kss to obtain $\frac{\partial a_{ij}}{\partial K_{ss}}$ . Multiply by $\frac{\partial \zeta}{\partial a_{ij}}$to get the damping sensitivity for the two elements $\frac{\partial \zeta}{\partial a_{ij}} \frac{\partial a_{ij}}{\partial K_{ss}}$. The total sensitivity is the summation of the two individual mode sensitivities.

The damping ratio after applying the change in the gain should be:

New damping ratio = Old damping ratio +(damping sensitivity with respect to Kss)× ΔKss

Table (3.3) presents the expected results and the actual results of the simulation.

Table 3.3 Using the Damping Sensitivity to Improve the Modes Damping

| Mode | Old damping ratio | (damping sensitivity with respect to Kss) × ΔKss | Calculated new damping ratio (addition result) | Resulting new damping ratio (simulation result) |
|---|---|---|---|---|
| -0.740±6.159i | 0.1193 | -0.0013 | 0.118 | 0.1179 |
| -1.137±2.879i | 0.3673 | 0.0028 | 0.3701 | 0.3701 |

Calculated damping sensitivities conclude that, changing the gain value by 0.5 will improve the damping of low frequency oscillations by 0.28% while the damping of high frequency oscillations will drop by 0.13%. As seen, the expression for damping sensitivity calculation was

perfectly able to compute the new damping ratio when applying predefined change to Kss. Thus, the novel damping sensitivity method can potentially be used to calculate the required change in the PSS parameters to get a desired damping ratio.

Above was done for all PSS parameters. Tables (3.4) and (3.5) show the damping sensitivity with respect to T1 and T2 for $\Delta T1= 1$ and $\Delta T2= 0.01$.

Table 3.4 Using the Damping Sensitivity to Improve the Modes Damping

| Mode | Old damping ratio | (damping sensitivity with respect to T1) × $\Delta T_1$ | Calculated new damping ratio (addition result) | Resulting new damping ratio (simulation result) |
|---|---|---|---|---|
| -0.740±6.159i | 0.1193 | 0.0033 | 0.1226 | 0.1224 |
| -1.137±2.879i | 0.3673 | -0.0044 | 0.3629 | 0.3629 |

Table 3.5 Using the Damping Sensitivity to Improve the Modes Damping

| Mode | Old damping ratio | (damping sensitivity with respect to T2) × $\Delta T_2$ | Calculated new damping ratio (addition result) | Resulting new damping ratio (simulation result) |
|---|---|---|---|---|
| -0.740±6.159i | 0.1193 | -0.00005 | 0.1192 | 0.1192 |
| -1.137±2.879i | 0.3673 | 0.00005 | 0.3673 | 0.3673 |

The change in $T_2$ has been made deliberately small. It should be noticed that, the change of T2 and T4 in each step should be relatively small to avoid the nonlinearity produced by the differentiations $\frac{\partial a_{ij}}{\partial T_2}$ and $\frac{\partial a_{ij}}{\partial T_4}$ (due to these parameters location in the denominator).

As a change in specific parameter can cause contradictory effect on the system modes, counterbalancing by other parameters should be considered to get the possible maximum damping for all modes.

The PSS parameters tuning was automated for the two modes by setting:

$$H = \begin{bmatrix} \frac{\partial \zeta_1}{\partial a_{ij}}\frac{\partial a_{ij}}{\partial T_1} & \frac{\partial \zeta_1}{\partial a_{ij}}\frac{\partial a_{ij}}{\partial T_2} & \frac{\partial \zeta_1}{\partial a_{ij}}\frac{\partial a_{ij}}{\partial T_3} & \frac{\partial \zeta_1}{\partial a_{ij}}\frac{\partial a_{ij}}{\partial T_4} & \frac{\partial \zeta_1}{\partial a_{ij}}\frac{\partial a_{ij}}{\partial K_{ss}} \\ \frac{\partial \zeta_2}{\partial a_{ij}}\frac{\partial a_{ij}}{\partial T_1} & \frac{\partial \zeta_2}{\partial a_{ij}}\frac{\partial a_{ij}}{\partial T_2} & \frac{\partial \zeta_2}{\partial a_{ij}}\frac{\partial a_{ij}}{\partial T_3} & \frac{\partial \zeta_2}{\partial a_{ij}}\frac{\partial a_{ij}}{\partial T_4} & \frac{\partial \zeta_2}{\partial a_{ij}}\frac{\partial a_{ij}}{\partial K_{ss}} \end{bmatrix} \quad \text{and} \quad \Delta P = \begin{bmatrix} \Delta T_1 \\ \Delta T_2 \\ \Delta T_3 \\ \Delta T_4 \\ \Delta K_{ss} \end{bmatrix}$$

Then, the required change in PSS parameters to meet predefined change in the damping of mode k is:

$$\begin{bmatrix} \Delta\zeta_1 \\ \Delta\zeta_2 \end{bmatrix} = [H].\Delta P \tag{3.93}$$

The system shown in equation (3.93) however is over determined; there are infinite combinations of ΔP which can be used to control the damping. Since only two oscillatory modes exist (a control mode associated with $E'_q$ and $E_{fd}$ and a local mode associated with δ,ω) only two degrees of freedom are needed to tune the PSS. The question becomes how are these two control parameters selected out of the possible five choices (T1, T2, T3, T4 and Kss)? The approach adopted here was to give each of these an opportunity to contribute by updating them one at a time. Thus, we start with T1 and write, for the two modes:

$$\begin{bmatrix}\Delta\zeta_1\\ \Delta\zeta_2\end{bmatrix} = \begin{bmatrix}\sum_{i,j}\frac{\partial\zeta_1}{\partial a_{ij}}\frac{\partial a_{ij}}{\partial T_1}\\ \sum_{i,j}\frac{\partial\zeta_2}{\partial a_{ij}}\frac{\partial a_{ij}}{\partial T_1}\end{bmatrix}.\Delta T_1 \tag{3.94}$$

$$[\Delta\zeta] = [H].\Delta T_1$$

Then:

$$\Delta T_1 = (H^T.\ H)^{-1}.\ H^T[\Delta\zeta] \tag{3.95}$$

Similar equations are written to update $\Delta T_2$, $\Delta T_3$, $\Delta T_4$ and $\Delta Kss$, each in turn.

The damping improvement step $\Delta\zeta_i$ for each mode is determined by subtracting the actual mode damping $\zeta_i$ from a general damping target $\zeta_{des}$, i.e.:

$$\Delta\zeta_i = \zeta_{des} - \zeta_i \tag{3.96}$$

The damping steps should be made sufficiently small for the incremental calculus to be correct. Thus if the maximum value of $\Delta\zeta_i$ is, say, larger than 0.01 (1% damping), then all $\Delta\zeta$ are adjusted using:

$$[\Delta\zeta] = \frac{[\Delta\zeta]}{\max([\Delta\zeta])}\times 0.01 \tag{3.97}$$

Another useful technique is to add a weight to a particular mode, such that the improvement process will favor it over other modes thus:

$$\Delta\zeta_i = (\zeta_{des} - \zeta_i)\times weight \tag{3.98}$$

Where the relative weight determines the degree of improvements in the damping ratio among the modes. This is particularly helpful when the updating process favors particular modes due to their higher relative sensitivity.

Mentioned techniques were used to update the PSS parameters and the results demonstrate that the maximum damping for the two modes can be achieved when:

T1 = 1.4396 T2 = 0.015 T3 = 1.41 T4 = 0.015 Kss=0.6537

These parameters yield:

Table 3.6 Oscillatory Modes and Damping Ratios After Tuning the PSS Parameters

| Modes | Damping Ratio |
|---|---|
| -1.8144±6.0554i | 0.287 |
| -0.8943±2.9847i | 0.287 |

### 3.4.2.4 PSS Transfer Function and Bode Diagram

Referring to equation (3.82), designed power system stabilizer has the transfer function:

$$G_{PSS}(s) = Kss * \frac{1 + sTN_1 + s^2TN_2}{1 + sTD_1 + s^2TD_2}$$

Conventional method is to attempt to design a PSS function which is the inverse of the generator and excitation system transfer function to insure that the added electrical torque component is in phase with the rotor deviation. Other methods involve using the eigenvalues sensitivity to shift the real part of the mode to the left side of s-plane based on equation (3.56).

Our novel method operates directly on the damping of the mode using damping sensitivity as explained in the last section. For further validation, the bode diagrams of the PSS before and after the tuning process were plotted as shown in figure (3.11). Obviously, tuned PSS using the damping sensitivity calculation offers a strong phase/gain characteristics for frequencies in the range of interest.

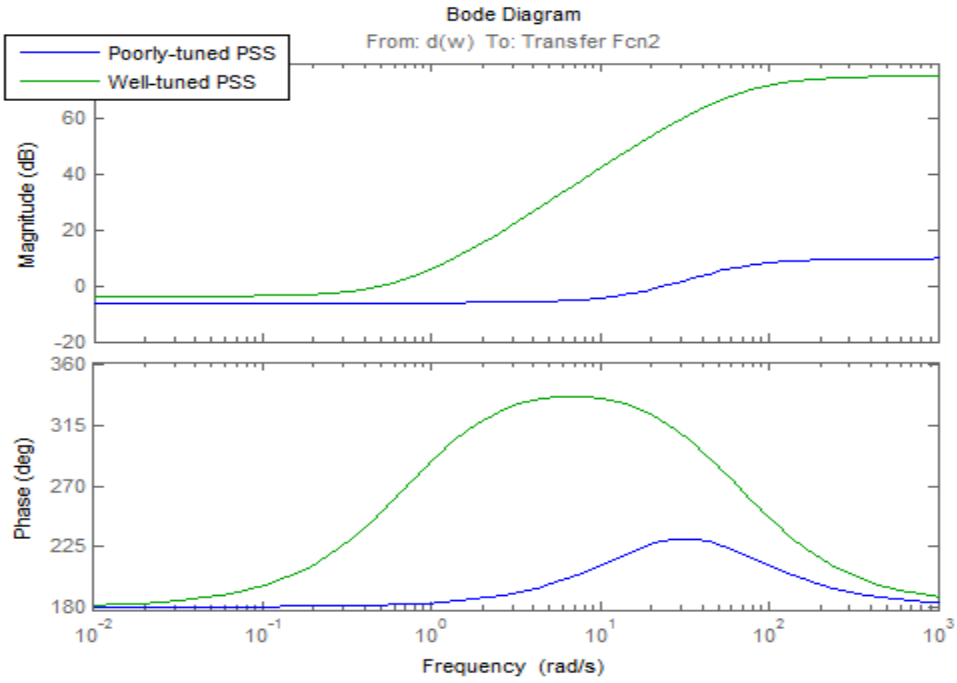


Figure 3.11 Bode Diagram of the Designed PSS

The overall frequency characteristic of the system (from Δω to Pe) is presented in the next section

### 3.4.2.5 Well-Tuned and Poorly Tuned PSS

Figure (3.12) shows the MATLAB Simulink model of the single machine infinite bus system that has been constructed using equations defined in section 3.3.1. Updated values of the power system stabilizer parameters have been calculated using the damping sensitivity calculation method. New values applied to the model to plot the zero-pole map and the bode diagram.

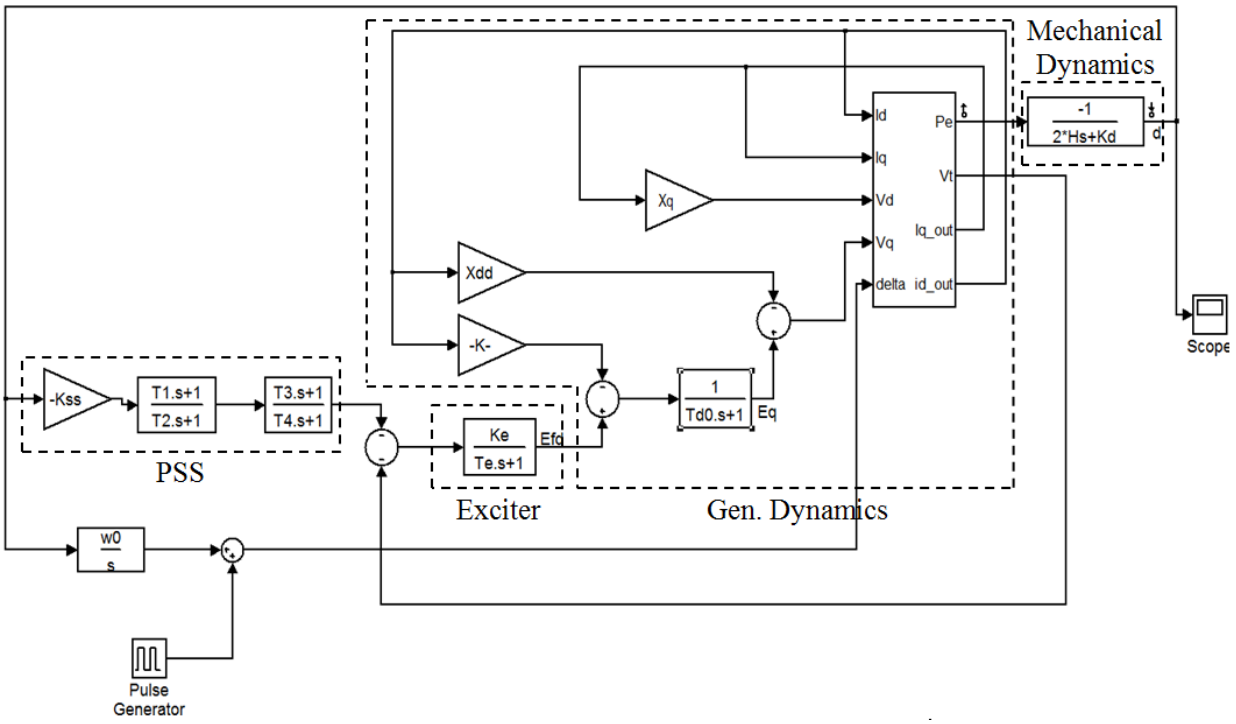


Figure 3.12 Simulink Model of the Single Machine Infinite Bus System

The model defines $\Delta\omega$ as an input linearization point and $P_e$ as an output linearization point. To attain the frequency response of the system, the dynamics of all other machines should be disabled. That can be done by defining $\Delta\omega$ as constant. It should also be noticed that, there are two paths between $\Delta\omega$ and $P_e$; the first one pass through the PSS while the other presents the angle dynamics. To display the effect of the tuned PSS on the system, the angle dynamics path should be removed as can be seen in figure (3.13)

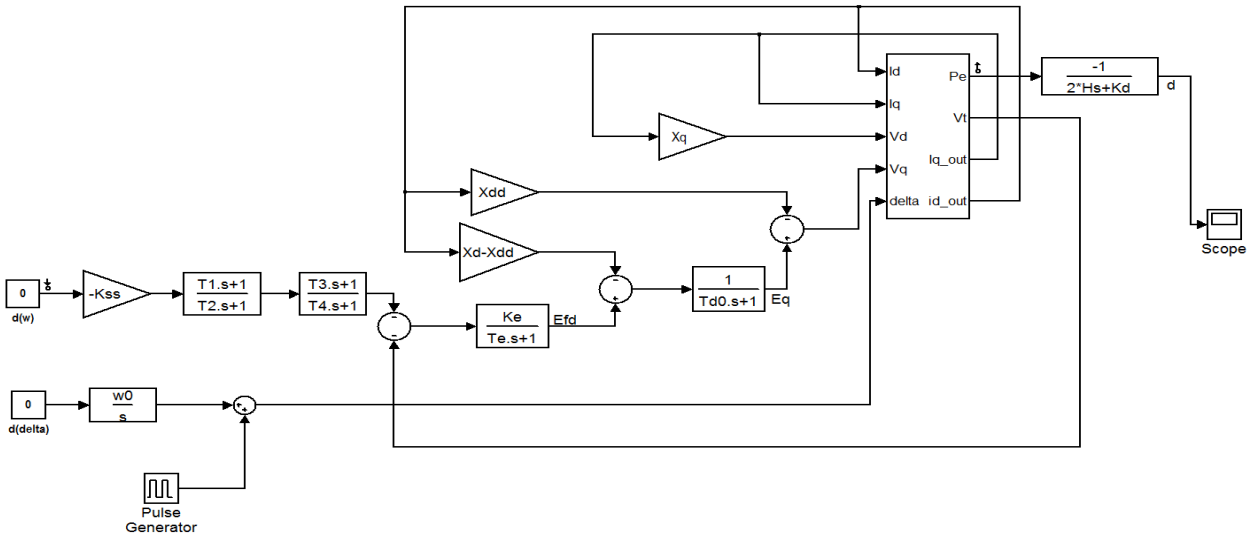


Figure 3.13 Machine Infinite Bus System with Removed Angle Dynamics Path

Superposition rule can be used to solve this problem. Separating the output power of the speed dynamics and the output power of the angle dynamics makes it possible to monitor each path distinctly.

Superposition technique has been exercised on the model and the result revealed in figure (3.14)

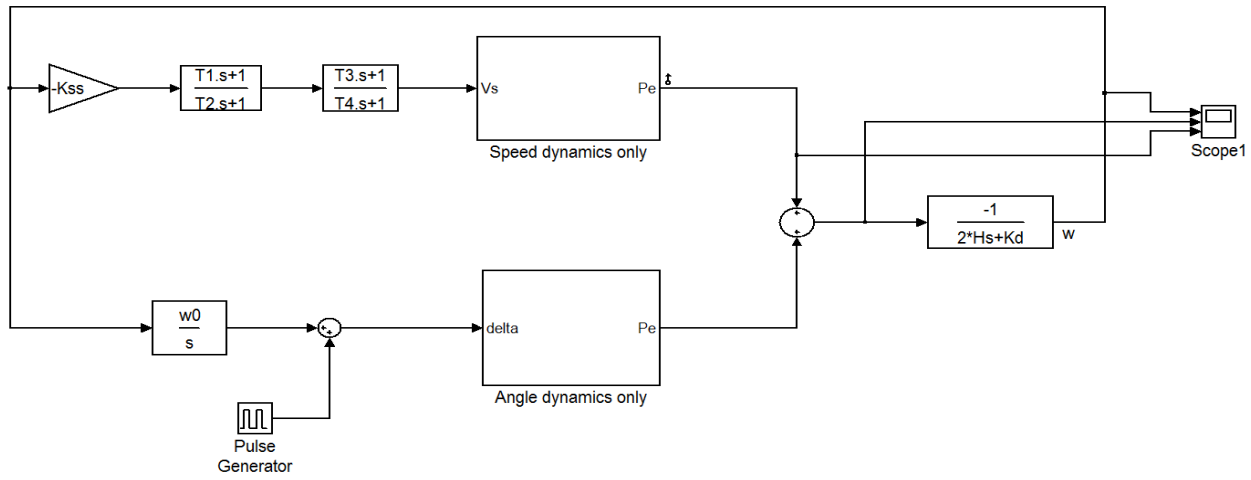


Figure 3.14 Superposition Exercised on the Single Machine Infinite Bus System

The results of the small signal analysis before and after tuning the power system stabilizer have been subjected to the comparison. Table (3.8) displays the modes, damping ratios, the phase and the gain before and after the tuning process. Figure (3.15) presents the pole-zero map before and after tuning the PSS respectively. Figure (3.16) shows the bode plot diagram for the two cases as well.

Table 3.7 Comparison Between Poorly Tuned PSS and Well-Tuned PSS

| | eigenvalue | Damping Ratio % | Magnitude dB | Phase deg |
|---|---|---|---|---|
| Before Tuning PSS | -0.740±6.159i | 0.1193 | -17.9 | -135 |
| | -1.137±2.879i | 0.3673 | -4.19 | -87.8 |
| After Tuning PSS | -1.814±6.055i | 0.2870 | 21.6 | 2.28 |
| | -0.894±2.984i | 0.2870 | 22.8 | 45.3 |

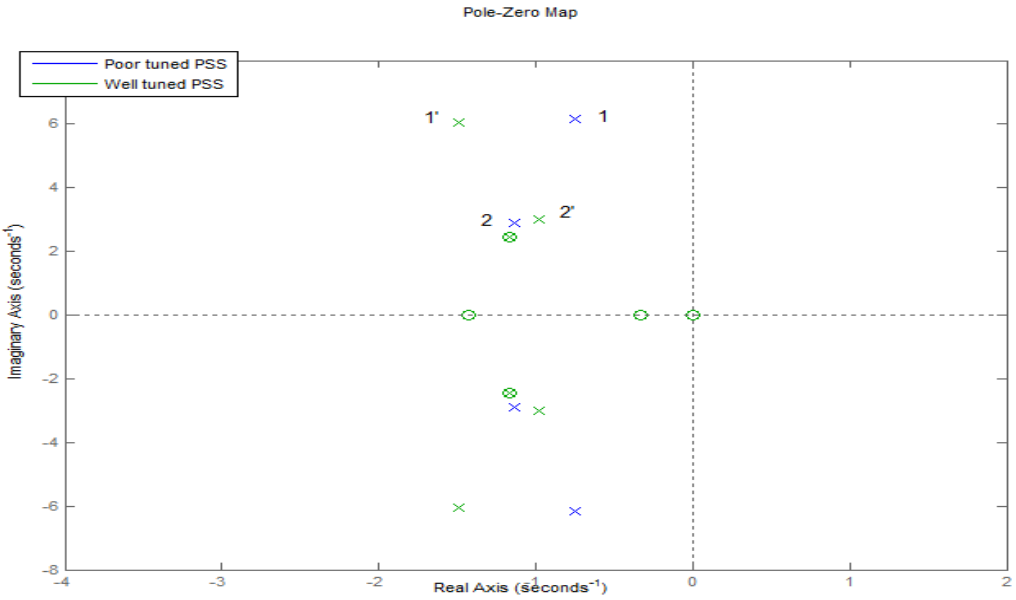


Figure 3.15 Pole-Zero Map of Poorly-Tuned PSS and Well-Tuned PSS

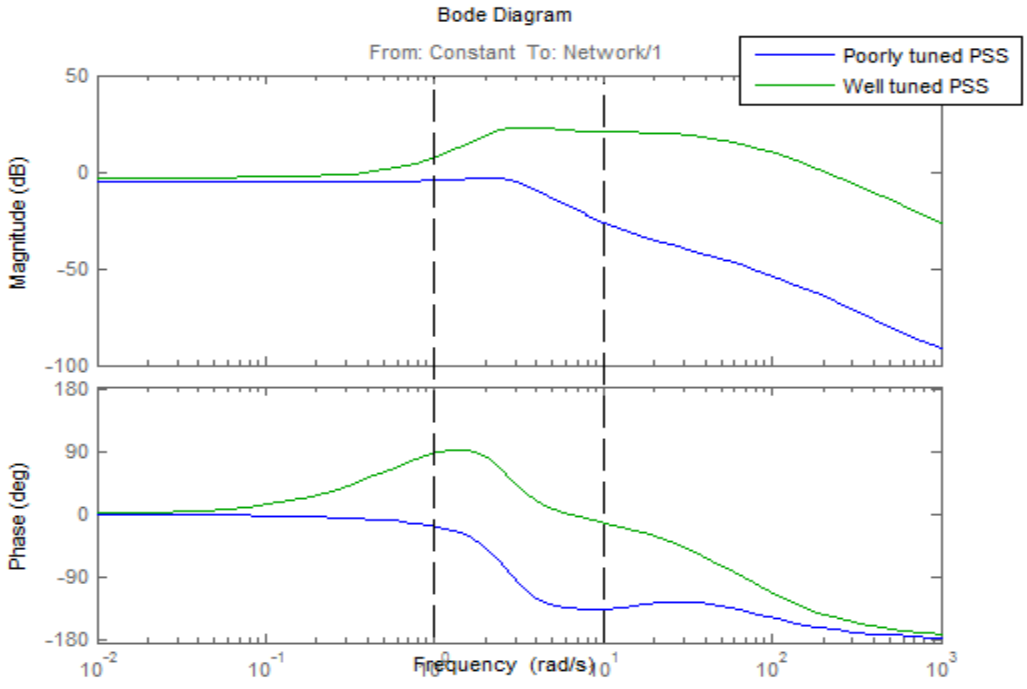


Figure 3.16 Bode Diagram of Overall PSS-Pe System for Poorly Tuned and Well-Tuned PSS

Pole zero map shows that the oscillatory mode (mode.1) has improved by 16.77%. The damping sensitivity approach to tune the PSS parameters was successful to move it to the left from location 1 to location 1'. On the other hand, control mode (mode.2) was degraded slightly. Figure (3.16) shows the magnitude/frequency characteristics of the overall PSS-$P_e$ system. Marked region (between 1-10 rad/s) is the region of interest. For these frequencies, well-tuned PSS was able to provide required phase shift especially for the high frequencies (mode.1) with a strong damping gain.

Speed deviation, deviations in total electrical power and the output power of the speed dynamics plotted respectively for the system before tuning the PSS and after the tuning process. Results in figures (3.17) and (3.18) present noticeable declining in the oscillations frequency.

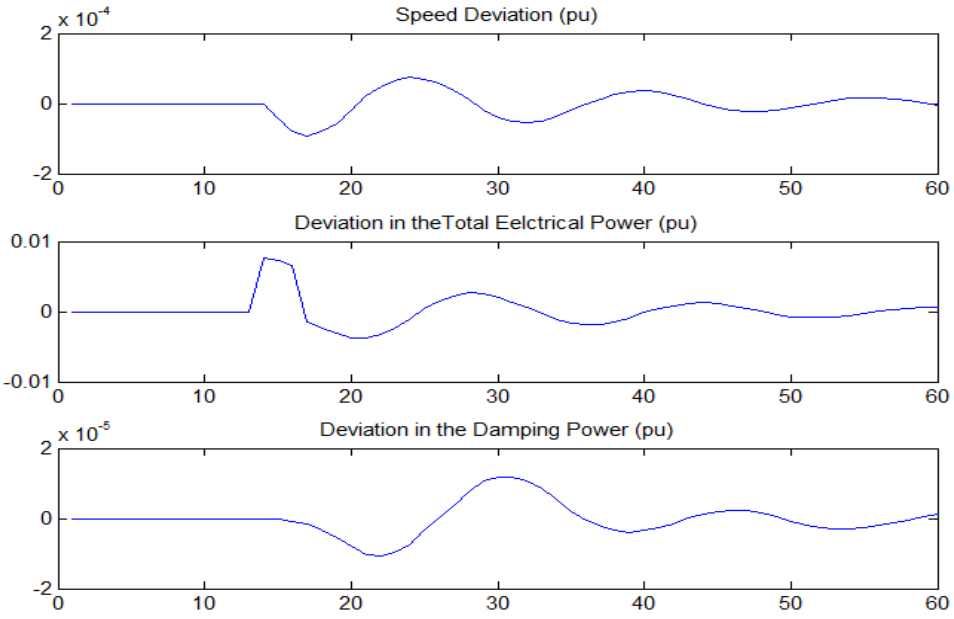


Figure 3.17 Speed, Total Electrical Power and the Damping Power for Poorly-Tuned PSS

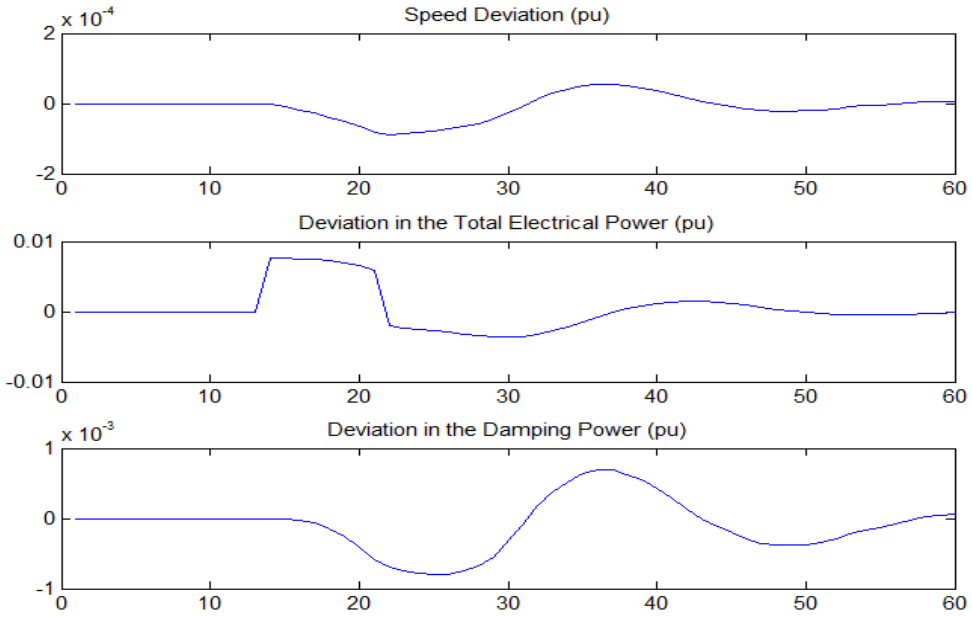


Figure 3.18 Speed, Total Electrical Power and the Damping Power for Well-Tuned PSS

### 3.5 The Procedure of Tuning the Power System Stabilizers Using the Damping Sensitivity Calculation

1. Use the system, generators and load data to build the admittance matrix. Eliminate non generating buses and find the conductance and susceptance matrices.
2. Set initial values for the PSS parameters.
3. Set the DampStep to be a small value which increases through an iterative procedure until it reaches predefined maximum damping value (30-40%). Starting with a small value of DampStep allows starting with the weakest mode to improve it first.
4. Build the state matrix A of the system (including the PSS) as explained in section 3.3.1. Eliminate non-state variables.
5. Calculate the eigenvalues and the damping ratios.

6. Define the elements that are functions of the PSSs parameters and store their locations in the state matrix. The number of these elements depends on the number of installed PSSs in the system.
7. For these elements, calculate $\frac{\partial a_{ij}}{\partial T_1}$, $\frac{\partial a_{ij}}{\partial T_2}$, $\frac{\partial a_{ij}}{\partial T_3}$, $\frac{\partial a_{ij}}{\partial T_4}$, and $\frac{\partial a_{ij}}{\partial K_{ss}}$.
8. Detect the weakest mode. Calculate the damping sensitivity $\frac{\partial \zeta_k}{\partial a_{ij}}$ of that mode using equation (3.61)
9. For all elements that are functions of T1, calculate $\frac{\partial a_{ij}}{\partial T_1} * \frac{\partial \zeta_k}{\partial a_{ij}}$, find the summation of these values and store it in the first column of the matrix $\frac{\partial \zeta}{\partial P}$. Repeat with respect to T2, T3, T4 and Kss.
10. Define $\Delta\zeta$ as the difference between the DampStep and the actual damping of the mode. To keep $\Delta\zeta$ smaller than predefined value (1%), use equation (3.97). Moreover, to favor a particular mode, give it higher weight than other modes.
11. Use the weak modes detected in equation (3.95) to update the PSS parameters starting with T1 and using as many as desired to increase degrees of freedom. The minimum number of parameters should be equal to number of under-damped modes.
12. Increase the value of DampStep and repeat from step 4. Monitor the number of detected weak modes and accordingly, use as much as required of the PSS parameters to solve equation (3.95)
13. Repeat until all the damping ratios of all modes become higher the predefined maximum damping value or no more improvement is possible.

CHAPTER 4

RESULTS AND DISCUSSION

To test the proposed method, two systems were used: Kundur's two-area four-machine system and the IEEE 9-Bus system.

## 4.1 Two-Area Four-Machine System

Figure (4.1) show the two-area four-machine system. The system consists of two identical areas linked by two 230KV lines. Each area has two 900MVA /20KV round rotor generators. Complete system data are tabulated in Appendix A

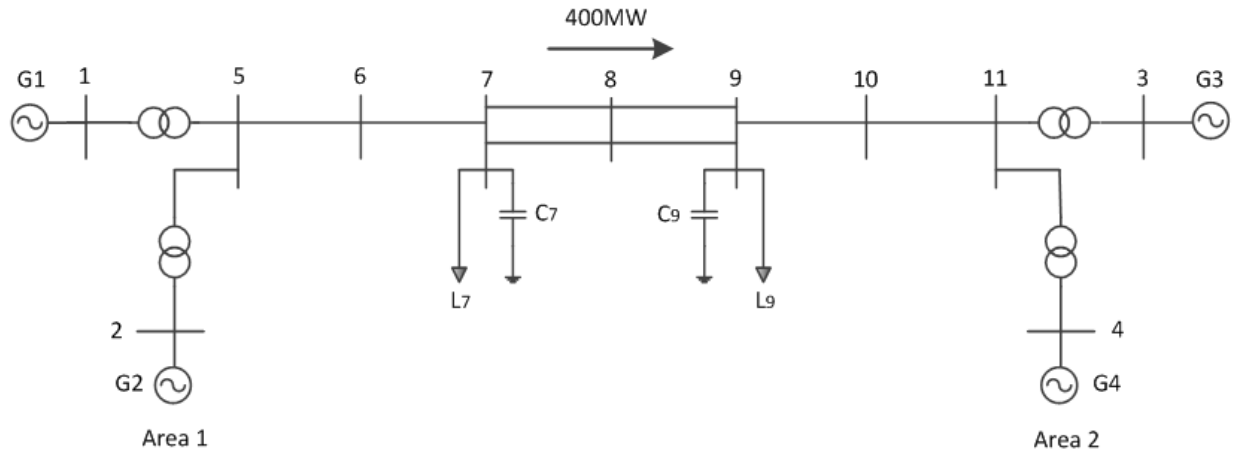


Figure 4.1 Two-Area Four-Machine System

### *4.1.1 Small Signal Stability Analysis*

The MathWorks, Inc. team has built a Simulink model of the two-area four-machine system to study the performance of three PSS for inter-area oscillations. The example analyzes the system behavior in four cases; without PSS, with Multi-Band PSS, with conventional Delta-Omega PSS from P. Kundur and with conventional acceleration power (Delta-Pa) PSS.

Small signal analysis of the system without PSS displayed undamped oscillatory modes leading to instability as shown by figures (4.2) and (4.3).

Figure (4.2) presents the positive sequence voltage (pu) at buses 7 and 9 and the active power (MW) transferred from bus 7 to bus 9. In the other hand, figure (4.3) shows Δδ (deg), speed (pu), acceleration power (pu) and the terminal voltage (pu).

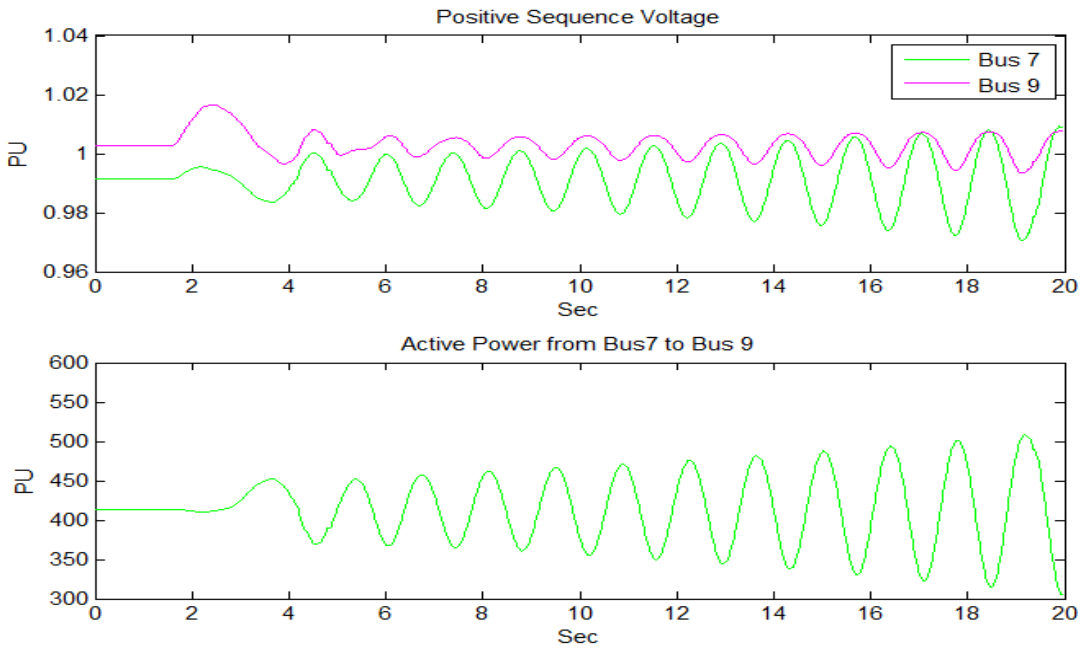


Figure 4.2 System Oscillations

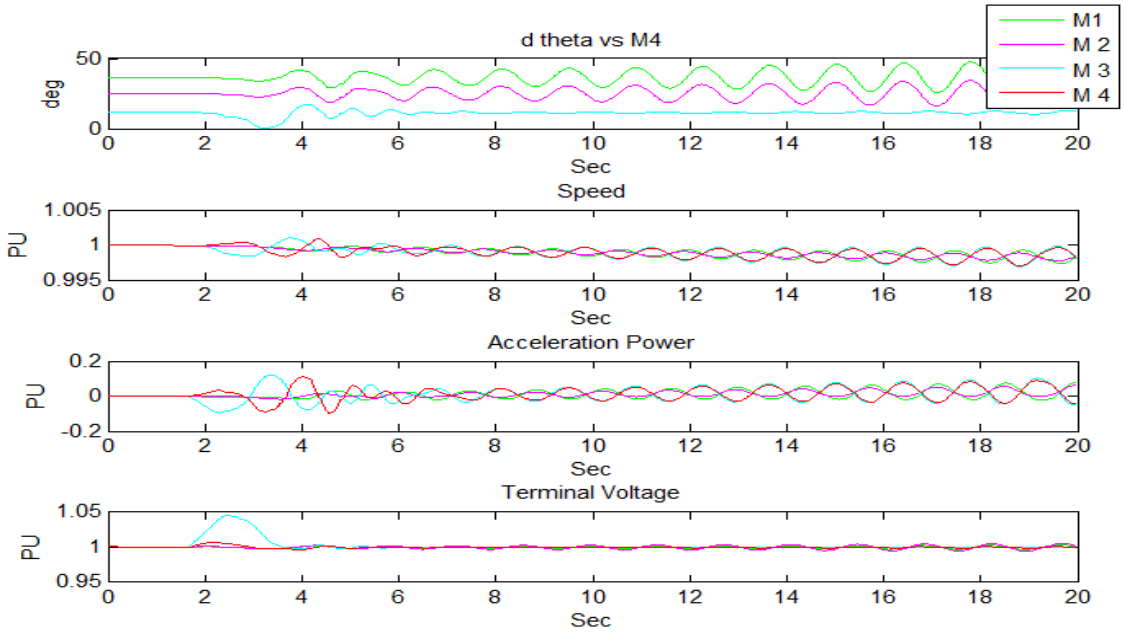


Figure 4.3 Machines Oscillations

MATLAB Linear analysis tool was used to plot the model pole-zero map as presented in figure (4.4). It shows one unstable mode at 3.9 rad/s and two poorly damped modes at 6.7 rad/s and 7.1 rad/s.

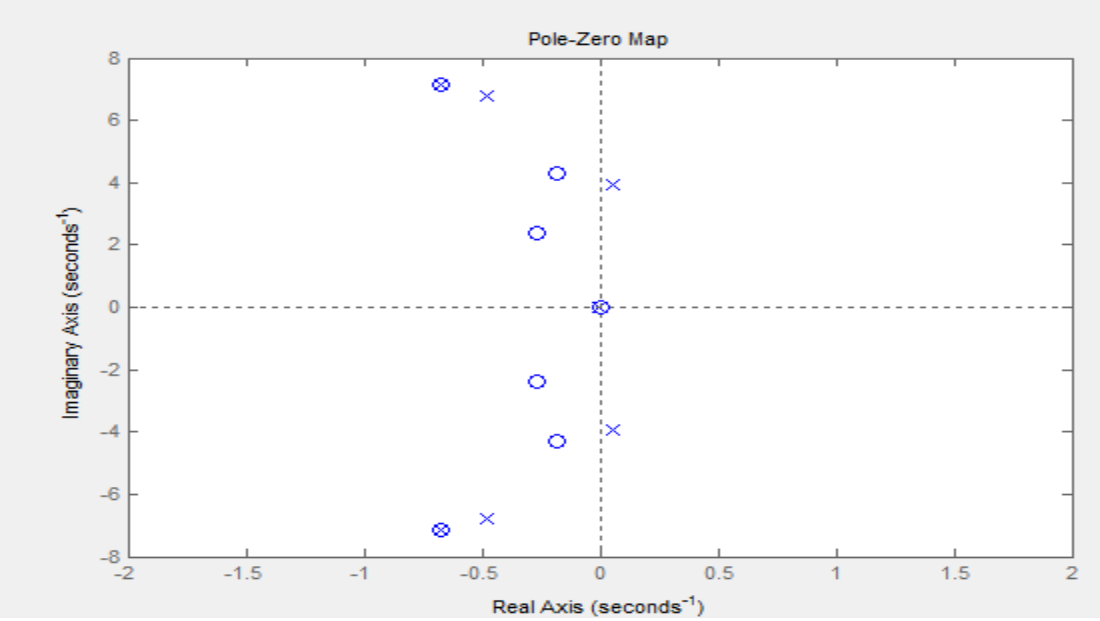


Figure 4.4 Pole-Zero Map of the System

MATLAB script was written and succeeded to obtain the same oscillatory modes. Table (4.14) presents these un-damped oscillatory modes and damping ratios resulting from the Simulink model and the MATLAB script.

Table 4.1 Modes and Damping Ratios Resulting from the MATLAB Script and the Simulink Model

| MATLAB Script | | Simulink Model | | |
|---|---|---|---|---|
| Mode | Damping Ratio (pu) | Mode | Damping Ratio (pu) | Area |
| 0.030±3.93i | -0.007 | 0.055±3.93i | -0.014 | Inter-area mode |
| -0.342±6.09i | 0.056 | -0.483±6.78i | 0.071 | Local mode(Area 1) |
| -0.366±6.30i | 0.057 | -0.677±7.13i | 0.095 | Local mode(Area 2) |

Simulink model modes have damping ratios slightly different than those resulting from the MATLAB script. The reason behind these differences is that the Simulink machine model is a detailed and complex non-linear model while the MATLAB script presents the machine by a simple first order model. Though, both the Simulink model and the MATLAB script show one un-damped inter-area mode and two local modes.

### *4.1.2 Power System Stabilizer Tuning*

Using the procedure explained in section 2.4, the MATLAB script was used to tune the parameters of the four PSSs installed in the four machines. The four PSSs were designed to have identical parameters. The initial values of the parameters were:

T1= 0.05  T2=0.02  T3=0.05  T4=0.02  Kss=30

The script was run and produced results approved that the new damping sensitivity method succeeds to improve the system damping as following:

Table 4.2 Modes and Damping Ratios After Applying and Tuning PSSs

| Mode | Damping Ratio (pu) | Area |
|---|---|---|
| -2.765±2.662i | 0.720 | Inter-area mode |
| -7.810±10.292i | 0.604 | Local mode(Area 1) |
| -8.113±10.817i | 0.600 | Local mode(Area 2) |

The inter-area mode damping has improved noticeably from being unstable to have a damping ratio of 72%. The damping of local modes has also improved. The parameters of the PSSs were updated as follows:

T1= 0.04519688  T2=0.01955181  T3=0.04519688  T4=0.01955181  Kss=47.7242

### *4.1.3 Comparison of Two Power System Stabilizers*

The Simulink model compares between three power system stabilizers; MB-PSS, Delta-Omega PSS and Delta-Pa PSS. Since the MB-PSS and the Delta- Omega PSS have the same stabilizing signal (w), there were used for comparison.

The settings of MB-PSS bands were selected such that they provide zero phase shifts between 0.1 Hz and 5Hz. That is:

FL=0.2  KL=30  FI=1.25  KI=40  FH=12  KH=160

Conventional Delta- Omega PSS from Kundur was tuned as described in section (2.2) to compensate for the lag phase generated in the system. The applied parameters are:

T1= 0.05  T2=0.02  T3=3  T4=5.4  Kss=30

Parameters of the designed Delta-Omega PSS that calculated in the last section were applied.

The bode diagrams of the four types of PSS were plotted in one figure for assessment purposes. As seen in figure (4.5), in the frequency range of interest, MB-PSS provides good phase compensation with high damping gain. The conventional Delta-Omega PSS designed by Kundur shows zero phase compensation for a wide range of frequencies (0.2-2 Hz) which makes it not as effective as the MB-PSS. In the other hand, although the Delta Pa offers good phase advance for frequencies larger than 0.3 Hz, it has destabilizing effect at low frequencies range in addition to the low frequency gain. The conventional Delta-Omega PSS designed by the proposed novel method has good phase compensation accompanied with strong damping gain.

Phase compensation of the designed Delta-Omega PSS looks small in the range of 0.4-3 Hz yet, considering the time constant of the exciter (Te=0.001), the lag phase in the system is very small and does not need large reaction from the lead-lag phase blocks.

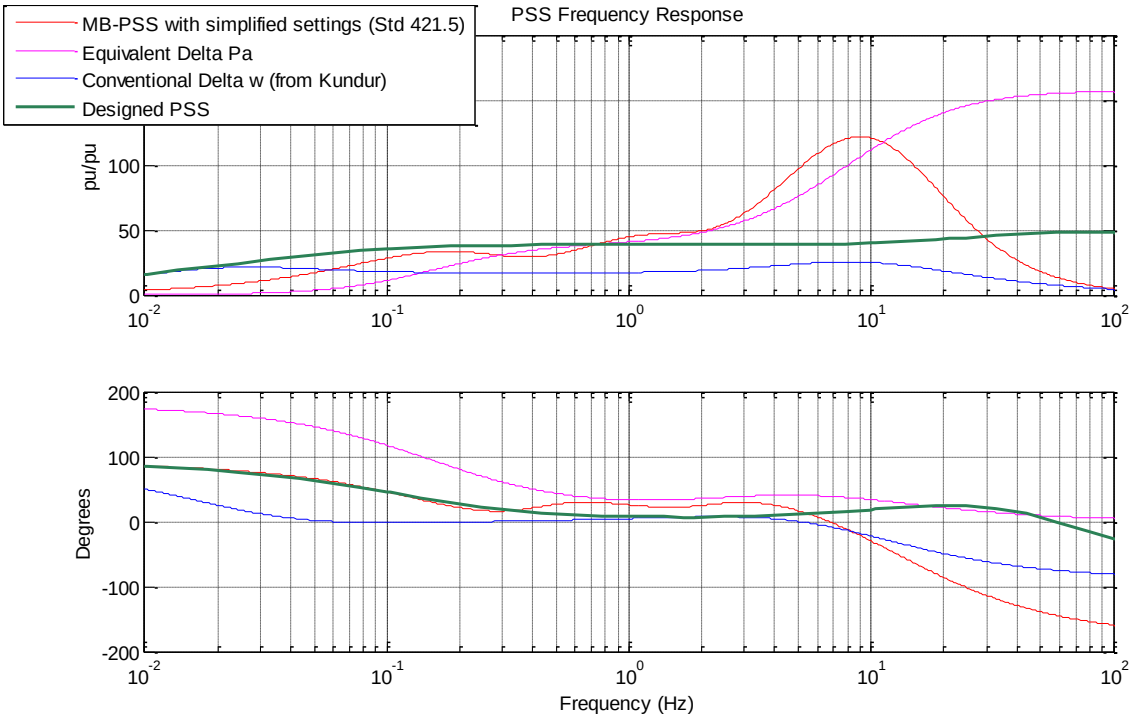


Figure 4.5 Bode Diagrams of Four Types of PSS

Since the MB-PSS has superiority over the Delta-Omega PSS designed by Kundur and the Delta-Pa PSS, it was used for further validation for the proposed PSS.

The bode diagram of the overall system including the PSS was plotted to examine the PSS efficiency to provide required phase compensation as presented in figure (4.6). It should be

mentioned that, to evaluate the ΔѠ-Pe transfer function the shaft dynamic should be disabled. That can be done by removing the feedback loop.

The bode diagram shows better characteristics at high frequencies when using designed Delta-Omega PSS although both PSSs agree in the frequencies of interest. Regarding to the damping gain, designed Delta-Omega PSS has superior gain characteristics.

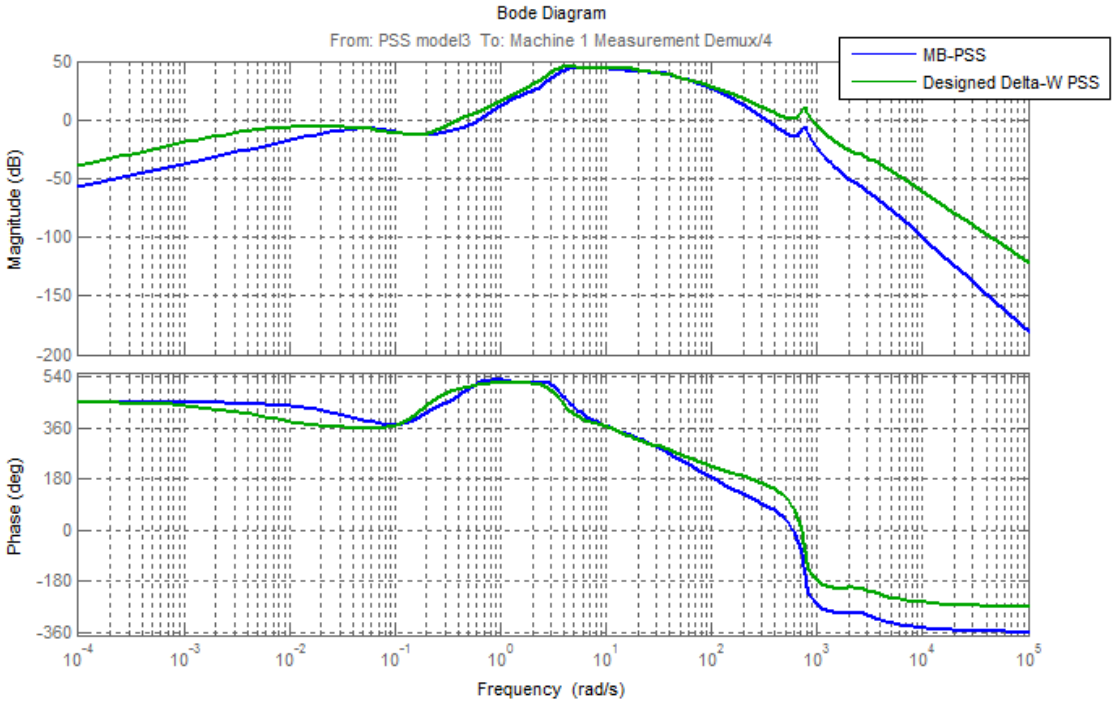


Figure 4.6 Bode Diagram of the Overall System Including the PSS

To evaluate the damping improvement, the pole-zero map has been modified slightly to show the same mode in case of No PSS, with MB-PSS and with designed Delta-Omega PSS.

The inter-area mode damping in the three cases presented in figure (4.7). Inter-area mode damping has been remarkably improved. The damping of the inter-area mode when applying the designed Delta-Omega PSS is 43% higher than its counterpart when applying the MB-PSS.

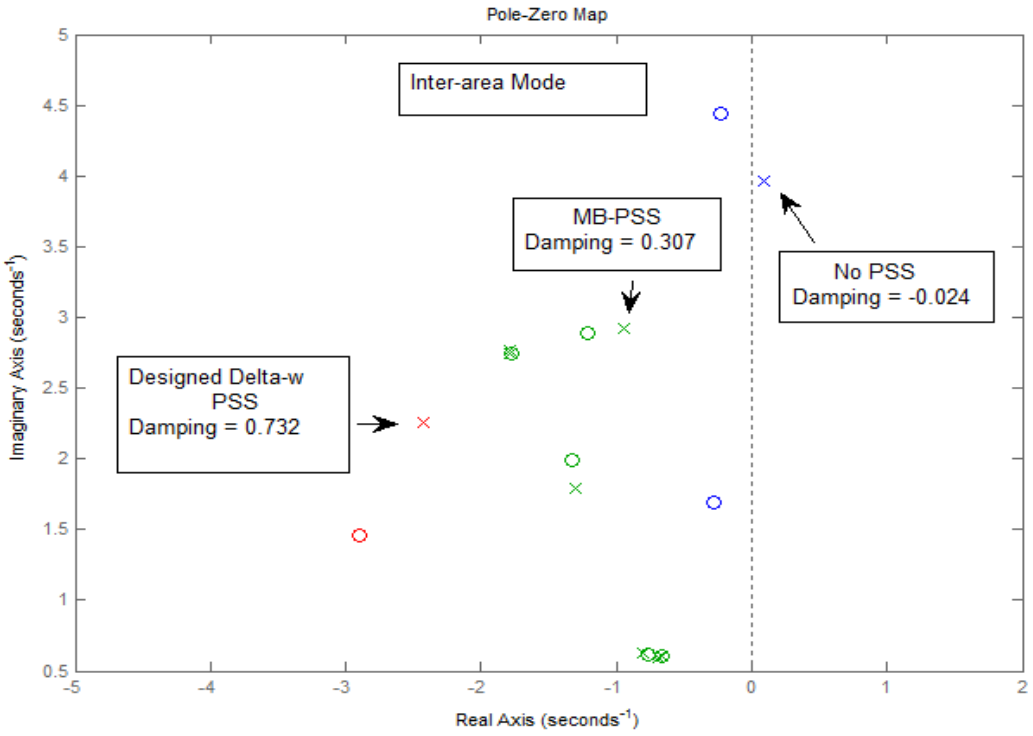


Figure 4.7 Damping of the Inter-Area Mode in Three Cases; No PSS, with MB-PSS and with Designed Delta-w PSS

Likewise, the damping of the local modes has been shown in figure (4.8). For these modes, pole-zero map shows damping ratios that are less than predicted by the MATLAB script. Again, that's because of the differences between the two systems.

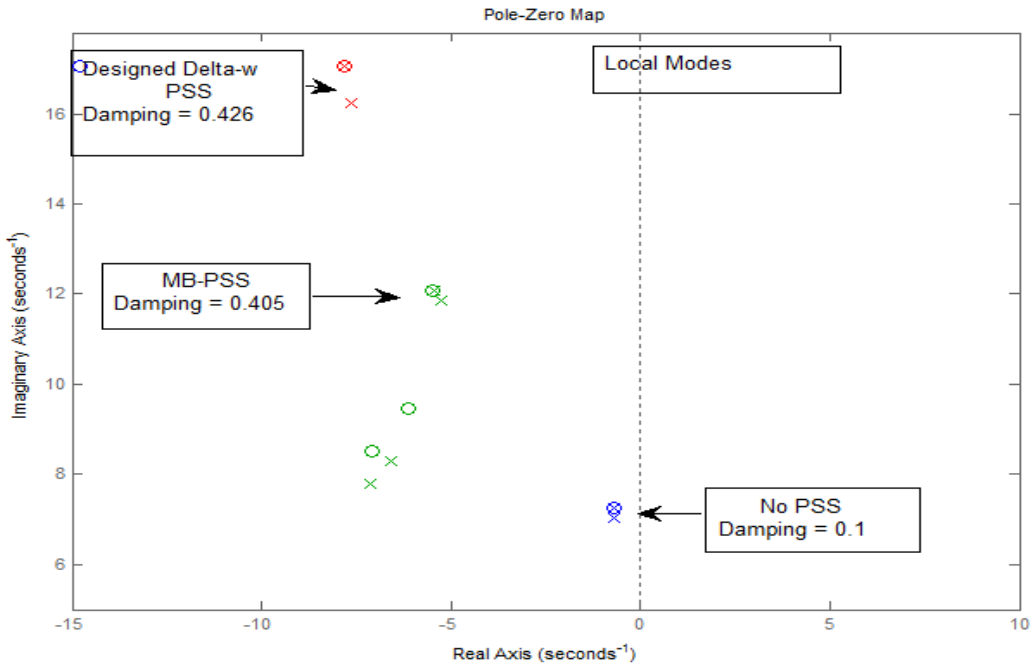


Figure 4.8 Damping of Local Modes in Three Cases; No PSS, with MB-PSS and with Designed Delta-w PSS

These results show that the designed Delta-Omega power system stabilizer using the damping sensitivity method did a good job damping the inter-area and local modes oscillation. It provided sufficient phase compensation to flatten the phase shift of the overall system.

Figures (4.9) and (4.10) display the simulated time-domain performance of the system and the synchronous machines when applying the MB-PSS while figures (4.11) and (4.12) show the effect of applying the designed Delta-Omega PSS.

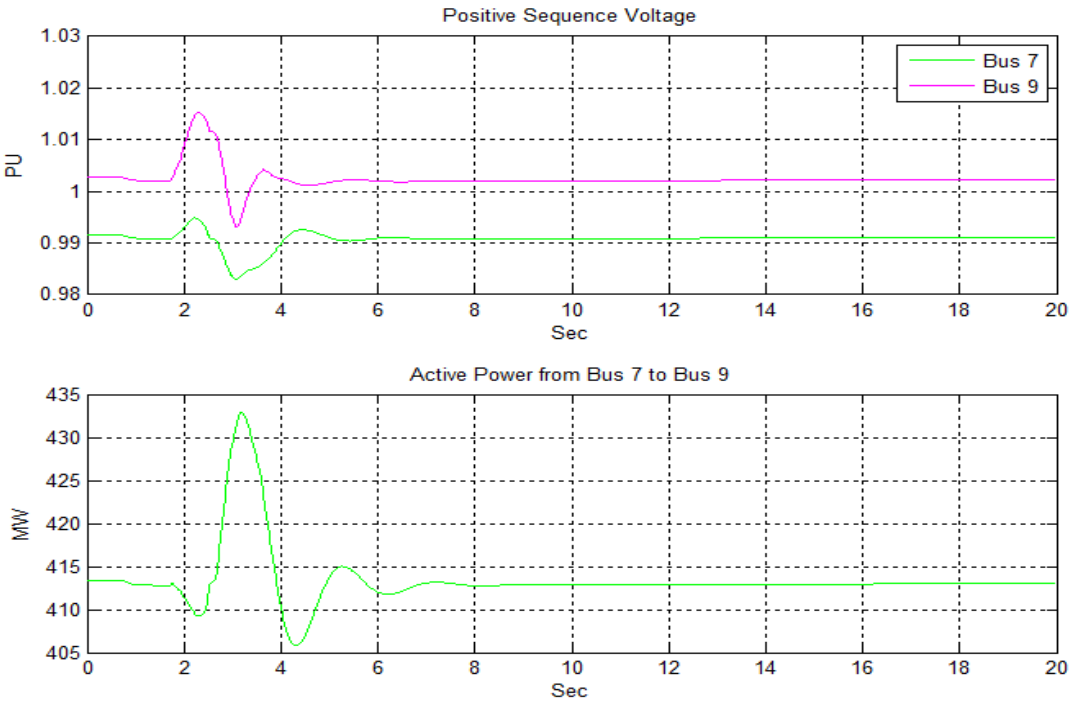


Figure 4.9 The Performance of the System When Applying the MB-PSS

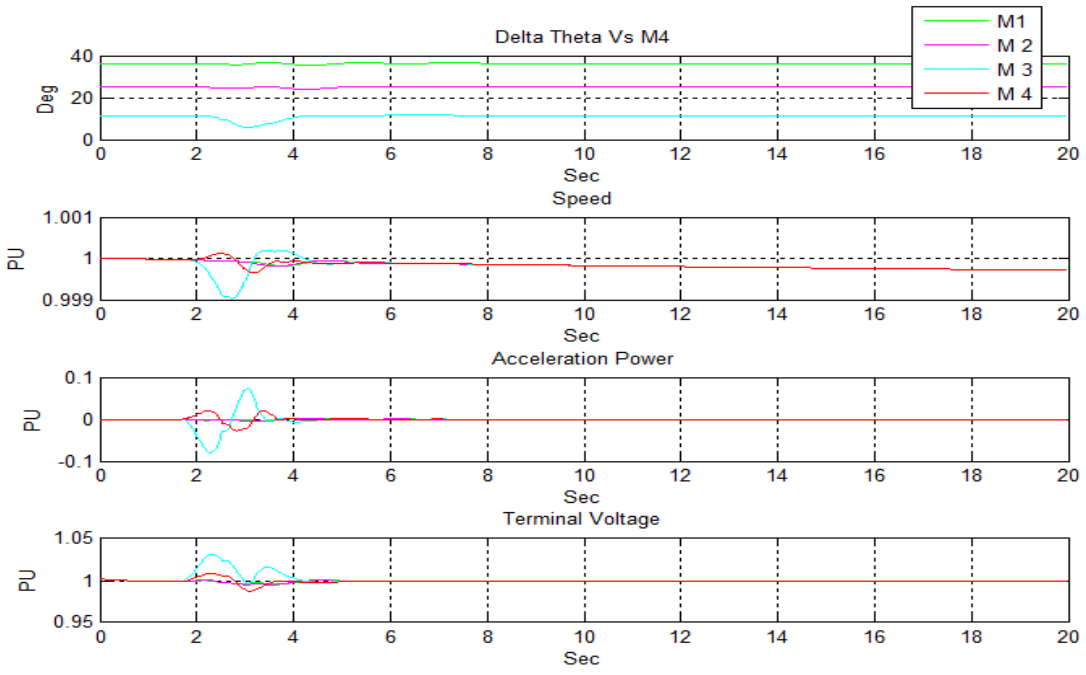


Figure 4.10 The Performance of the Synchronous Machines When Applying the MB-PSS

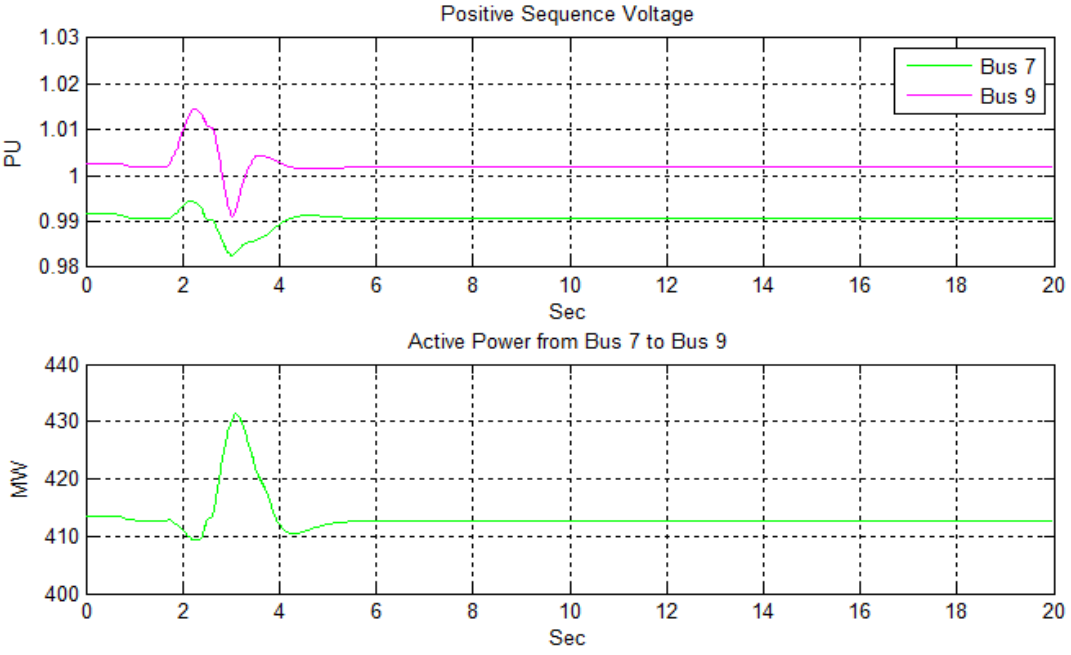


Figure 4.11 The Performance of the System When Applying the Designed Delta-Omega PSS

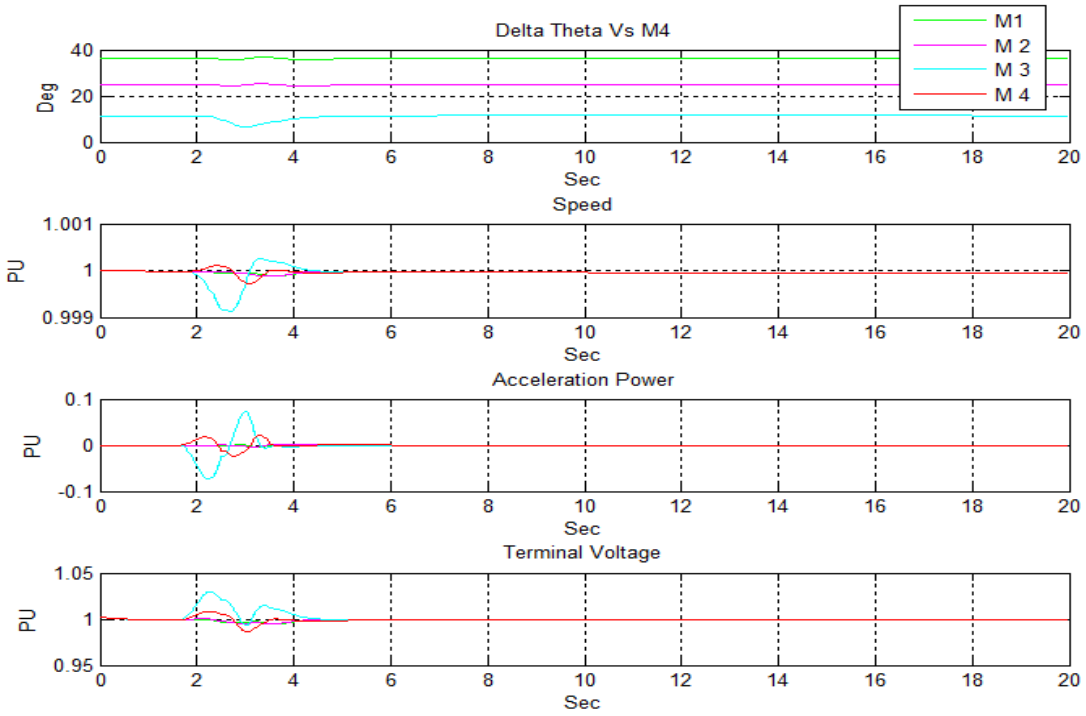


Figure 4.12 The Performance of the Synchronous Machines When Applying the Designed Delta-Omega PSS

Above figures show high degree of similarity between the results of applying the simple designed Delta-Omega PSS and the corresponding results when applying the complex MB-PSS. Though, designed Delta-Omega PSS provides better enhancement in the overall stability of the system. Figure (4.13) demonstrates the superiority of the designed Delta-Omega PSS over the MB-PSS in diminishing the overshooting and reducing the oscillations of the active power transferred from bus 7 to bus 9. Additionally, the designed Delta-Omega PSS helps the system to return to its equilibrium point in a shorter period of time.

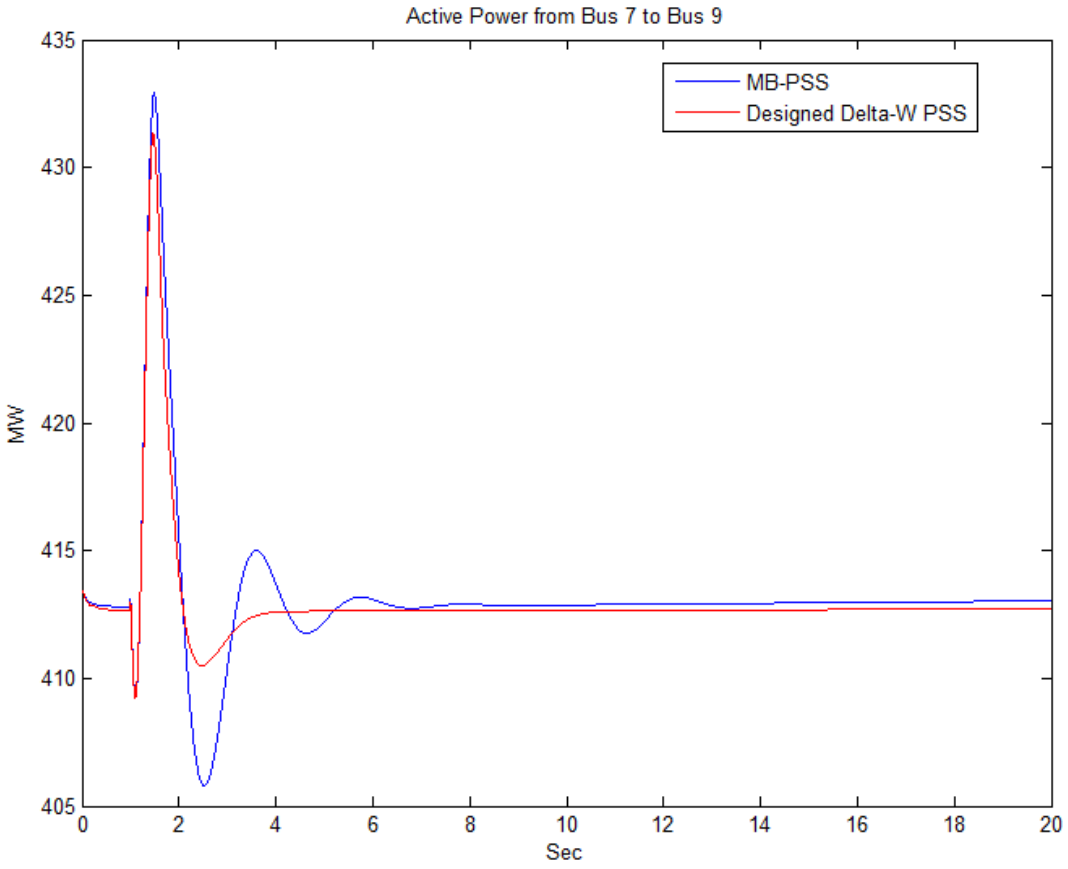


Figure 4.13 Comparison Between the MB-PSS and the Designed Delta-Omega PSS

### 4.2 IEEE9-Bus System

IEEE9-bus system presented by figure (4.14) consists of three synchronous machines connected to the transmission system through three transformers. The transmission system consists of six transmission lines with three constant power loads. The system data are presented in Appendix B.

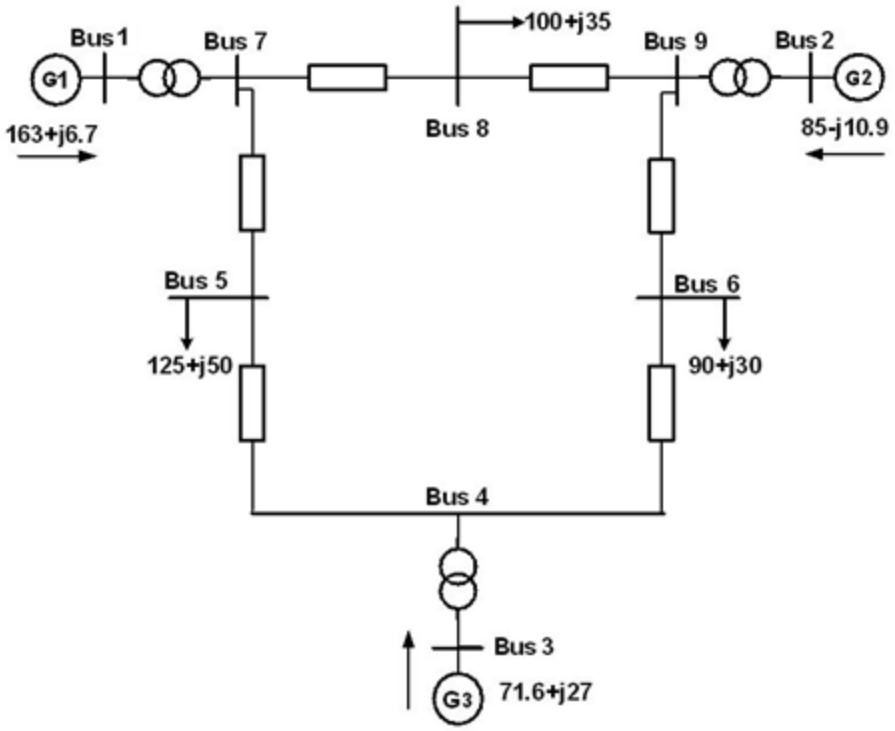


Figure 4.14 IEEE9-Bus System

### *4.2.1 Small Signal Stability Analysis*

The small signal response of the system to a step in the mechanical power is shown in figures (4.15) and (4.16). Figure (4.15) represents the oscillations in the active power of the three synchronous machines. On the other hand, figure (4.16) shows Δδ (deg), slip speed w.r.t center of inertia (pu), acceleration power (pu), and the terminal voltages (pu) of the three generators.

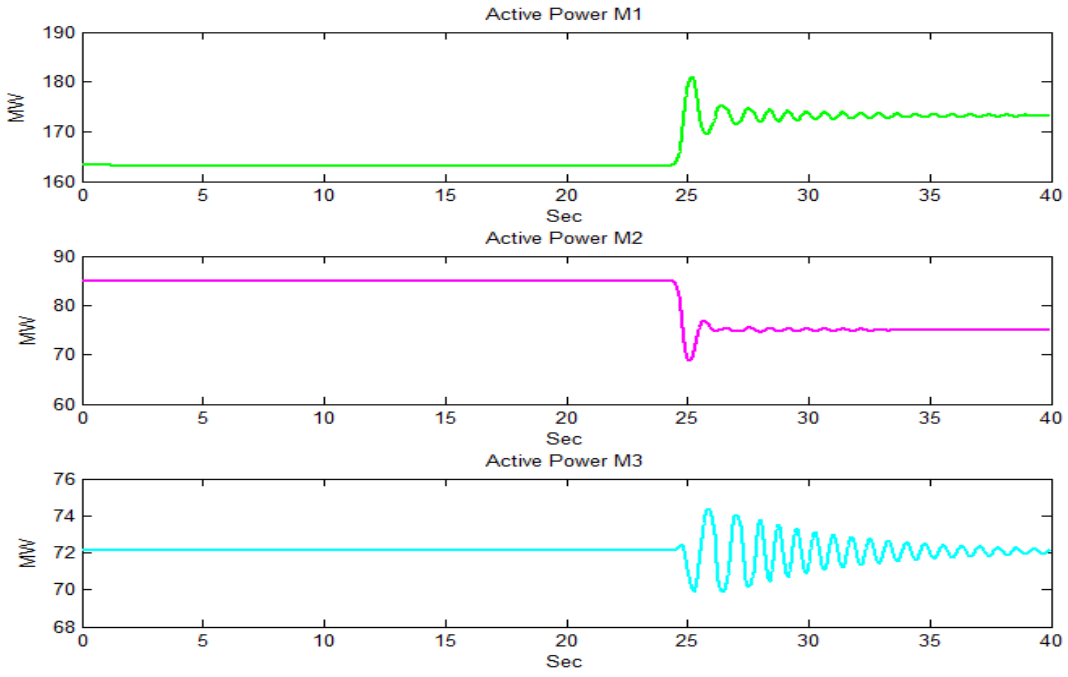


Figure 4.15 System Oscillations

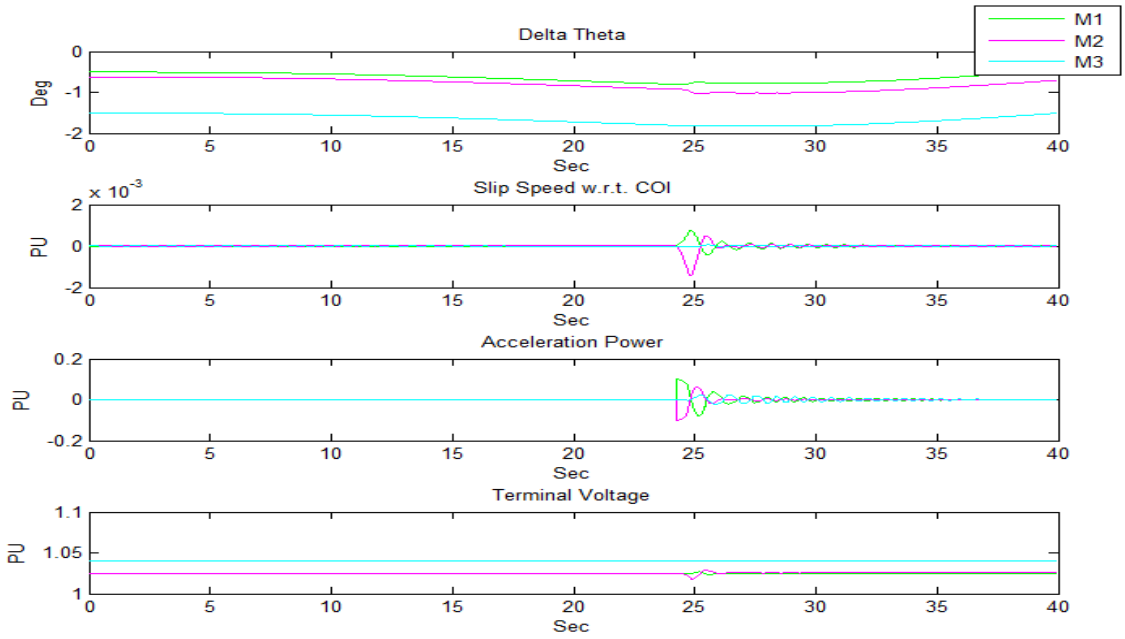


Figure 4.16 Machines Oscillations

A MATLAB script that described the system by simple first order differential equations was written and used to detect the oscillatory modes of the system. Table (4.3) presents the detected five oscillatory modes and damping ratios.

Table 4.3 Oscillatory Modes and Damping Ratios

| Mode | Damping Ratio (pu) |
|---|---|
| -9.992±21.873i | 0.41 |
| -9.999±13.639i | 0.59 |
| -7.620±10.022i | 0.60 |
| -2.802±10.588i | 0.25 |

| | |
|---|---|
| -0.233±7.795i | 0.03 |

### *4.2.2 Power System Stabilizers Tuning*

The proposed damping sensitivity method to tune the parameters of power system stabilizers were used to tune three power system stabilizers installed on the system generators. The three power system stabilizers have different parameters to increase the degree of freedom The initial values of the parameters of each generator were:

T1(1) = 0.05 T2(1) = 0.02 T3(1) = 0.05 T4(1) = 0.02 Kss(1) = 9

T1(2) = 0.05 T2(2) = 0.02 T3(2) = 0.05 T4(2) = 0.02 Kss(2) = 8

T1(3) = 0.05 T2(3) = 0.02 T3(3) = 0.05 T4(3) = 0.02 Kss(3) = 9

The tuning process was performed to increase the damping ratios of the two poorly damped modes. Results presented in table (4.4) show the achieved improvement.

Table 4.4 Modes and Damping Ratios After Applying and Tuning PSSs

| Mode | Damping Ratio (pu) |
|---|---|
| -15.136±24.794i | 0.52 |
| -12.170±19.018i | 0.53 |
| -6.921±13.062i | 0.46 |
| -3.645±6.103 | 0.51 |
| -3.645±6.103 | 0.51 |

The power system stabilizers parameters were updated as follow:

T1(1) = 0.00886 T2(1) = 0.0078 T3(1) = 0.00886 T4(1) = 0.0078 Kss(1) = 11.77

T1(2) = 0.0794 T2(2) = 0.00536 T3(2) = 0.0794 T4(2) = 0.00536 Kss(2) = 4.0288

T1(3) = 5.934 T2(3) = 0.6604 T3(3) = 5.934 T4(3) = 0.6604 Kss(3) = 0.435

### *4.2.3 The Performance of the System After Tuning the PSSs*

The system and machines performance in the time-domain presented in figures (4.17) and (4.18) prove the effectiveness of the tuned power system stabilizers in enhancing the overall system stability.

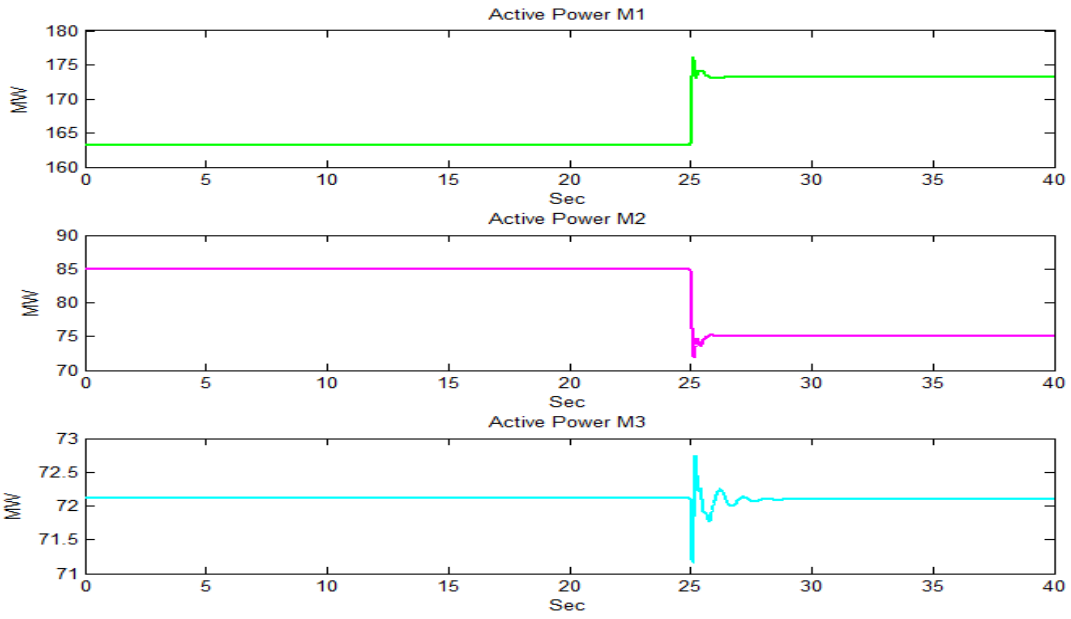


Figure 4.17 System Oscillations After Tuning the Power System Stabilizers

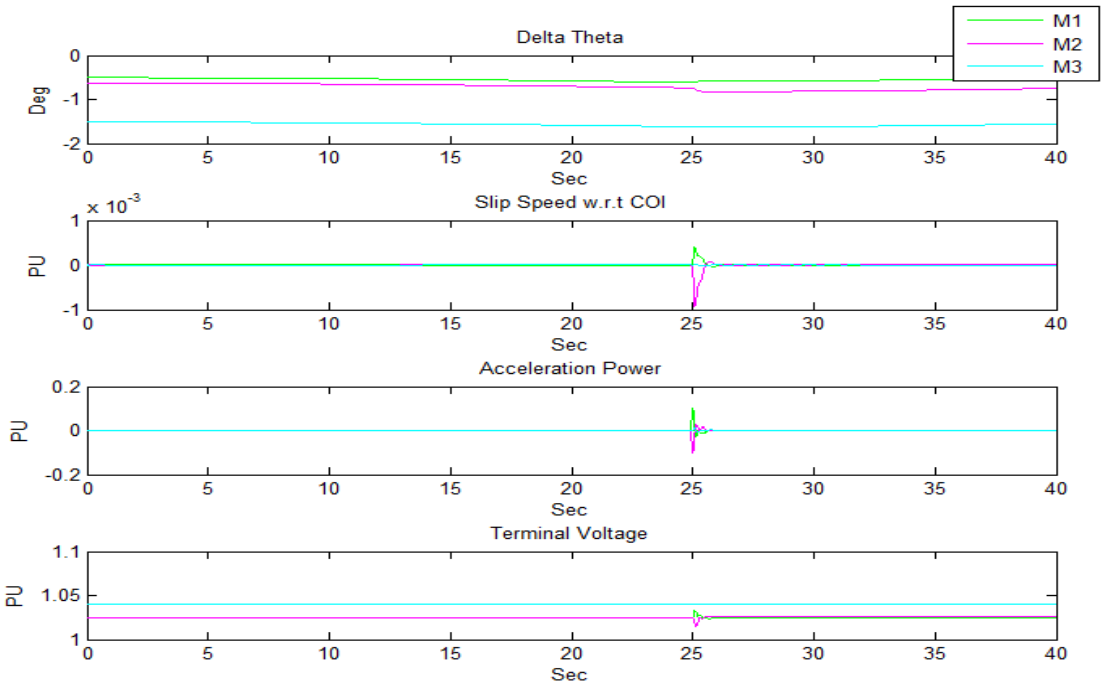


Figure 4.18 Machines Oscillations After Tuning the Power System Stabilizers

Achieved machines performance was compared to its counterpart when applying the power system stabilizer proposed by [9]. As [9], the transfer function of the system defined between the secondary voltage of the step up transformer and the terminal voltage using local measurements. Although the authors did not code a clear figure for the accomplished damping ratios, the speed waves shown in figures (4.19) and (4.20) confirm the superiority of the power system stabilizers that designed by this work. Gen.1 and Gen.2 correspond to Gen.(2) and Gen.(3) in [9] respectively.

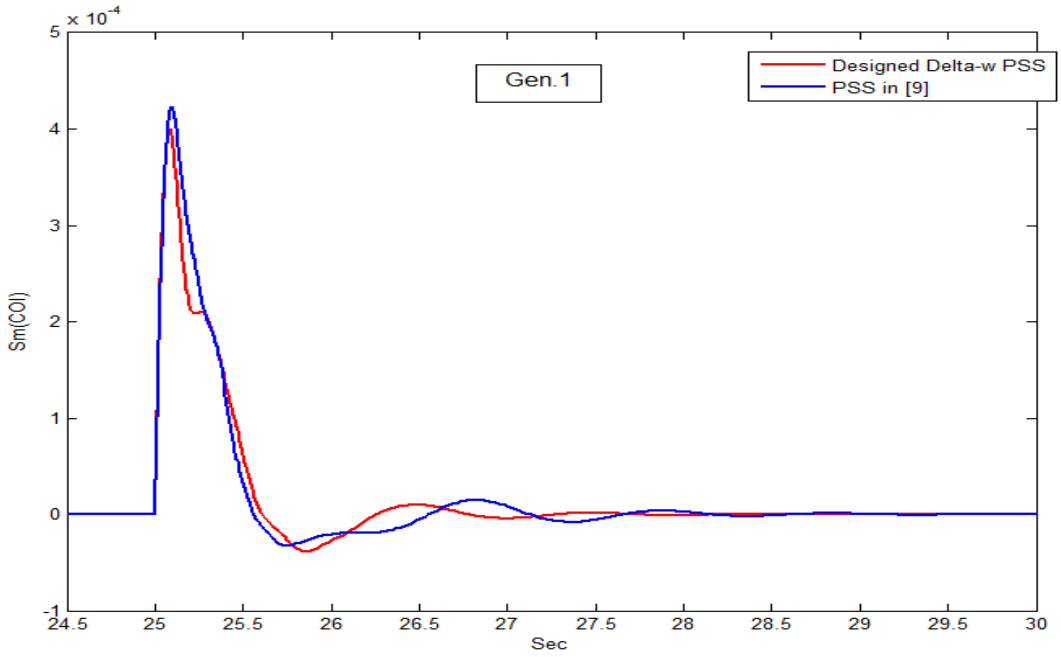


Figure 4.19 Slip Speed w.r.t Center of Inertia of Gen.1

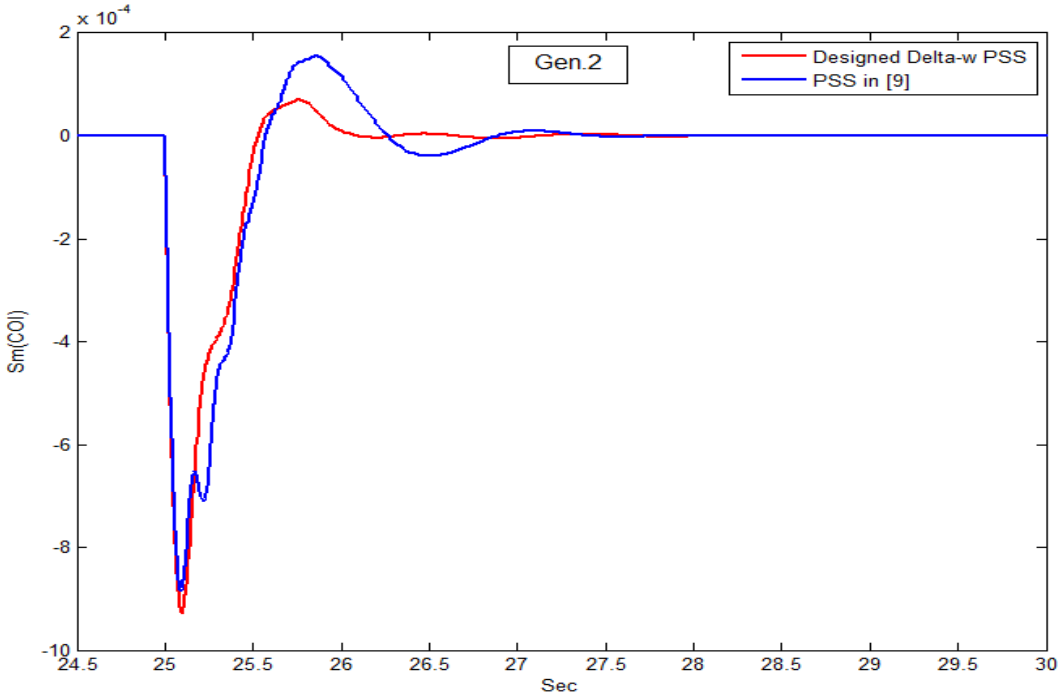


Figure 4.20 Slip Speed w.r.t Center of Inertia of Gen.2

# CHAPTER 5

# CONCLUSION

## 5.1 Conclusion

In this work, a novel method to tune the power system stabilizer parameters was developed. This method is based on an explicit expression for the damping sensitivity. The key advantage of the method is that it operates on the modes damping directly.

The proposed method was tested on the well-known two-area four-machine system and the IEEE9-Bus system to examine the performance of the designed power system stabilizer.

The small signal stability of the two-area four-machine system has been explored by virtue of frequency response analysis. Results presented a remarkable enhancement in the inter-area mode from being negatively damped to be a well-damped mode. Likewise, local modes experienced a decent damping improvement. The damping ratios of the poorly damped oscillatory modes of the IEEE9-Bus system were significantly improved

The performance of the overall system was assessed and effectiveness of the designed power system stabilizer to retrieve the system stability was verified.

For further validation, the results of the designed power system stabilizer were compared with complex and robust PSS designs. Although the designed power system stabilizer has simple structure, it showed high degree of robustness and effectiveness.

# REFERENCES


[1] D. Trudnowski, "Properties of the Dominant Inter-Area Modes in the WECC Interconnect ", ed, 2012.

[2] F. P. Demello and C. Concordia, "Concepts of synchronous machine stability as affected by excitation control," *IEEE Transactions on power apparatus and systems,* vol. 88, no. 4, pp. 316-329, 1969.

[3] M. J. Gibbard and D. J. Vowles, "Reconciliation of methods of compensation for PSSs in multimachine systems," *IEEE Transactions on Power Systems,* vol. 19, no. 1, pp. 463-472, 2004.

[4] H. Shi, C. Chen, and Y. Jin, "Sensitivity analysis of interconnected power system low frequency oscillation," in *Advanced Applications of Electrical Engineering*, Houston, USA, 2009, pp. 147-152: WSEAS Press.

[5] J. Zhang, C. Y. Chung, and Y. Han, "A novel modal decomposition control and its application to PSS design for damping interarea oscillations in power systems," *IEEE Transactions on power systems,* vol. 27, no. 4, pp. 2015-2025, 2012.

[6] M. Klein, G. J. Rogers, S. Moorty, and P. Kundur, "Analytical investigation of factors influencing power system stabilizers performance," *IEEE Transactions on Energy Conversion,* vol. 7, no. 3, pp. 382-390, 1992.

[7] P. Kundur, N. J. Balu, and M. G. Lauby, *Power system stability and control*. McGraw-hill New York, 1994.

[8] R. Grondin, I. Kamwa, G. Trudel, L. Gerin-Lajoie, and J. Taborda, "Modeling and closed-loop validation of a new PSS concept, the multi-band PSS," in *2003 IEEE Power Engineering Society General Meeting (IEEE Cat. No.03CH37491)*, 2003, vol. 3, pp. 1-1809 Vol. 3.

[9] A. Kumar, "Power system stabilizers design for multimachine power systems using local measurements," *IEEE Transactions on Power Systems,* vol. 31, no. 3, pp. 2163-2171, 2016.

# APPENDIX A

# TWO-AREA FOUR-MACHINE SYSTEM DATA

Table A.1 System Data (pu on 100MVA/230KV base)

| Element | From | To | Resistance (pu/km) | Inductance (pu/km) | Admittance (pu/km) | Length (km) |
|---|---|---|---|---|---|---|
| T-1 | 1 | 5 | 0.0 | 0.0167 | 0.0 | - |
| T-2 | 6 | 2 | 0.0 | 0.0167 | 0.0 | - |
| T-3 | 11 | 3 | 0.0 | 0.0167 | 0.0 | - |
| T-4 | 10 | 4 | 0.0 | 0.0167 | 0.0 | - |
| Line-1 | 5 | 6 | 0.0001 | 0.001 | 0.00175 | 25 |
| Line-2 | 6 | 7 | 0.0001 | 0.001 | 0.00175 | 10 |
| Line-3 (double line) | 7 | 8 | 0.0001 | 0.001 | 0.00175 | 110 |
| Line-4 (double line) | 8 | 9 | 0.0001 | 0.001 | 0.00175 | 110 |
| Line-5 | 9 | 10 | 0.0001 | 0.001 | 0.00175 | 10 |
| Line-6 | 10 | 11 | 0.0001 | 0.001 | 0.00175 | 25 |

Table A.2 Generators Data (pu on 900MVA/20KV base)

| | Generators Data | | | | | Exciters Data | |
|---|---|---|---|---|---|---|---|
| | $X_q$ | $X_d$ | $X'_d$ | H | $T_{d0}$ | $K_e$ | $T_e$ |
| Gen.1 | 1.7 | 1.8 | 0.3 | 6.5 | 8 | 200 | 0.001 |
| Gen.2 | 1.7 | 1.8 | 0.3 | 6.5 | 8 | 200 | 0.001 |
| Gen.3 | 1.7 | 1.8 | 0.3 | 6.175 | 8 | 200 | 0.001 |

| | | | | | | | |
|---|---|---|---|---|---|---|---|
| Gen.4 | 1.7 | 1.8 | 0.3 | 6.175 | 8 | 200 | 0.001 |

Table A.3 Generation Level

| | Active Power (MW) | Reactive Power(MVAR) | Terminal Voltage |
|---|---|---|---|
| Gen.1 | 700 | 91 | $1.05<20.72^0$ |
| Gen.2 | 700 | 117 | $1.05<10.5^0$ |
| Gen.3 | 719 | 82 | $1.05<-5.38^0$ |
| Gen.4 | 700 | 82 | $1.05<-16.03^0$ |

Table A.4 Loading Level

| | Active Power (MW) | Reactive Power(MVAR) | Shunt Capacitors Reactive Power (MVAR) |
|---|---|---|---|
| Load.7 | 967 | -87 | 200 |
| Load.9 | 1767 | -87 | 350 |

# APPENDIX B

# IEEE9-BUS SYSTEM DATA

Table B.1 System Data (pu)

| Element | From | To | Resistance (pu) | Inductance (pu) | Admittance (pu) |
|---|---|---|---|---|---|
| T-1 | 1 | 7 | 0.0 | 0.0625 | 0.0 |
| T-2 | 2 | 9 | 0.0 | 0.0586 | 0.0 |
| T-3 | 3 | 4 | 0.0 | 0.0576 | 0.0 |
| Line-1 | 4 | 5 | 0.01 | 0.085 | 0.176 |
| Line-2 | 4 | 6 | 0.017 | 0.092 | 0.158 |
| Line-3 | 5 | 7 | 0.032 | 0.161 | 0.306 |
| Line-4 | 6 | 9 | 0.039 | 0.17 | 0.358 |
| Line-5 | 7 | 8 | 0.0085 | 0.072 | 0.149 |
| Line-6 | 8 | 9 | 0.0119 | 0.1008 | 0.209 |

Table B.2 Generators Data (pu)

| | Generators Data | | | | | Exciters Data | |
|---|---|---|---|---|---|---|---|
| | $X_q$ | $X_d$ | $X'_d$ | H | $T_{d0}$ | $K_e$ | $T_e$ |
| Gen.1 | 0.8645 | 0.8958 | 0.1198 | 6.4 | 5.9 | 200 | 0.05 |
| Gen.2 | 1.2578 | 1.3125 | 0.1813 | 3.01 | 5.89 | 200 | 0.05 |
| Gen.3 | 0.0908 | 0.1455 | 0.0608 | 23.64 | 8.96 | 200 | 0.05 |

Table B.3 Generation Level

| | Active Power (MW) | Reactive Power(MVAR) | Terminal Voltage |
|---|---|---|---|
| Gen.1 | 163 | 67 | $1.025<9.3^0$ |
| Gen.2 | 85 | -109 | $1.025<4.7^0$ |
| Gen.3 | 72 | 27 | $1.04<0^0$ |

Table B.4 Loading Level

| | Active Power (MW) | Reactive Power(MVAR) |
|---|---|---|
| Load.5 | 125 | 50 |
| Load.6 | 90 | 30 |
| Load.8 | 100 | 35 |

# VITA

Miyada Ahmed was born in Riadh, Saudi Arabia, to the parents of Alnazeer and Zubaida. She spent 15 years of her childhood in Saudi Arabia with her family. Ms. Ahmed received her Bachelor of Science degree in electrical and electronics engineering –power system engineering- in 2010 from University of Khartoum in Khartoum, Sudan. After graduation, she joined different engineering companies as an electrical engineer. Ms. Ahmed worked for 5 years in the industrial field before accepting a graduate research assistantship offer from the University of Tennessee at Chattanooga to reward a Master of Science degree in Electrical Engineering. She was awarded her degree in August 2017.